Design and Validation of Cable-Driven Robots for Human Rehabilitation and Assistance

by

Davis Poole

A thesis submitted to the Graduate Faculty of
Auburn University
in partial fulfillment of the
requirements for the Degree of
Master of Science

Auburn, Alabama
May 10, 2025

Keywords: Haptics, Human and robot interaction, System design and control, Robot design, Supernumerary Limbs, Assistive Devices

Approved by

Chad G. Rose, Assistant Professor of Mechanical Engineering
Michael E. Zabala, Associate Professor of Mechanical Engineering
Kimberly B. Garza, Associate Professor of Health Outcomes Research and Policy

Abstract

Human and robot interaction is the key to improving the lives of many people around the world through rehabilitation, simulation, and performance enhancement.

To improve rehabilitation initiatives and provide patients and doctors with the means for episodic future thinking (EFT), implementation of virtual reality (VR) simulations and the rendering of internal impedances in those simulations is key. While previous research has explored external effects in these simulations (such as haptic interaction with a virtual object), internal avatar changes remain an open question. Given that current devices only generate external effects, it is extremely valuable to understand if those effects could be interpreted as internal ones. To assess this, Ideveloped a novel robotic system (Stiffness Emulation Robot, SER) and a new controller for an existing haptics glove (HaptX G1) and conducted a binary discretion experiment which reveals that most people can differentiate the two impedance types.

Alternatively, instead of providing simulation effects, robots can be used to increase human performance by manipulating how one interacts with the world. An example of this is in search-and-rescue litter carry groups, where long-distance carry of high-loads can impose significant stress on human fingertips, leading to grip fatigue and eventual failure. While there exists off-the-shelf means of alleviating this stress, a robotic device could provide additional advantages such as enabling/disabling to remain unobtrusive when not in use – a critical requirement in high-stakes environments. To achieve such performance, the Curling Artificial Soft ExoskeleTon (CASET) was developed. An experiment where participants held high loads to failure both with and without CASET revealed drastic performance increases, both in carry time and grip fatigue reduction.

Acknowledgments

I would like to thank my advisor, Dr. Rose, for his assistance in both my research and professional development, as well as the various labs and groups who have provided me with either test subjects or hardware during both the CASET and SER projects such as the Harrison College of Pharmacy, CARE and AUBE labs, and the Auburn I&RC.

Table of Contents

List of Figures

List of Tables

Chapter 1

Introduction

The study of haptics primarily involves the incorporation of a touch element in physical or virtual simulations. This can be achieved through many different methods, but the most popular is through the design and control of robotic devices for human interaction.

To create effective touch sensations, the development of appropriate technology for each individual simulation is necessary. For example, in a situation where a doctor may use a kinesthetic robot to conduct teleoperated surgery, accurate haptic feedback on minuscule scales is required [10]. Alternatively, more macro-scale environments such as VR gaming, task training in a simulated space [11], or episodic-future-thinking (EFT) for internally acting joint diseases could require higher force outputs at a lower accuracy in unique degrees of freedom.

Previous research has explored external effects in these simulations (such as haptic interaction with a virtual object), internal avatar changes remain an open question. Given that current devices only generate external effects, it is extremely valuable to understand if those effects could be interpreted as internal ones. To assess this, I developed a novel robotic system (Stiffness Emulation Robot, SER) and a new controller for an existing haptics glove (HaptX G1) and conducted a binary discretion experiment which reveals that most people can differentiate the two impedance types.

Alternatively, instead of providing simulation effects, robots can be used to increase human performance by manipulating how one interacts with the world. An example of this is in search-and-rescue litter carry groups, where long-distance carry of high-loads can impose significant stress on human fingertips, leading to grip fatigue and eventual failure. While there exists off-the-shelf means of alleviating this stress, a robotic device could provide

additional advantages such as enabling/disabling to remain unobtrusive when not in use – a critical requirement in high-stakes environments. To achieve such performance, CASET was developed. This device was tested in a validation experiment where participants

Developing the appropriate device for a human-robot interaction application requires a fundamental understanding of the use case, desired sensation/interaction, size/scale, and the amount of force required. Although this results in a wide array of varying robots developed for varying tasks, there is overlap between many concepts used to design, build, and test said robots.

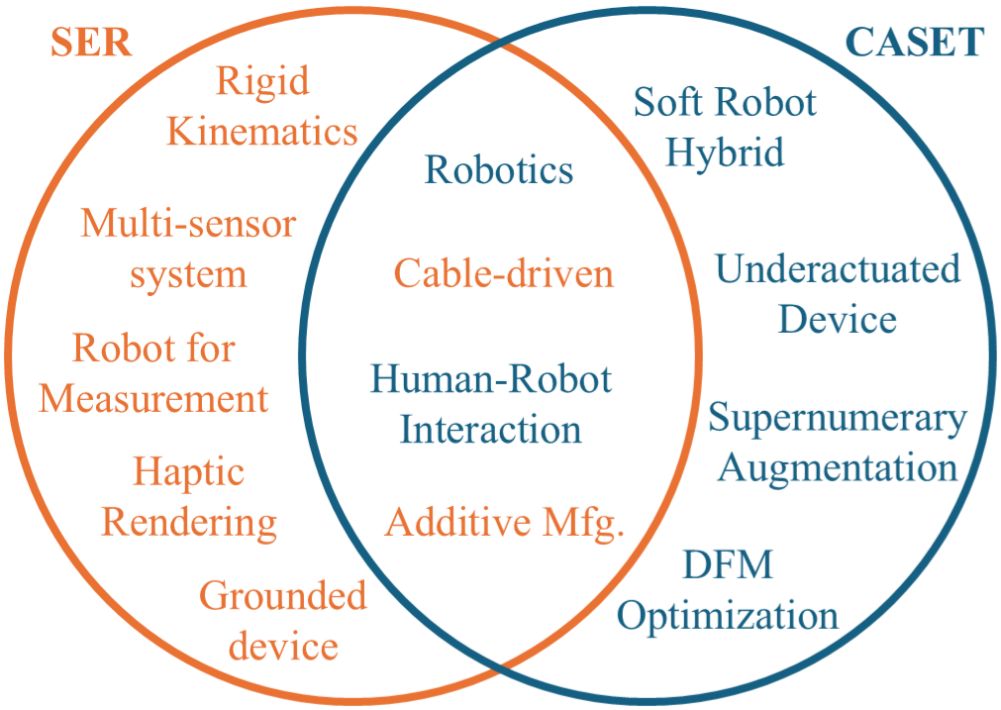

Figure 1.1: Overview of general concepts for both SER and CASET, with the overlap between devices shown. This paper will cover both the individual concepts for each device and the overlapping design principles.

This thesis explores robot design concepts through the development of two robots: CASET and SER. Each device was designed for a very different use, but both robots leverage overlapping concepts displayed in Fig. 1.1. Chapter 2 covers existing devices and reviews the design concepts displayed throughout the paper, Chapter 3 focuses on SER and the binary discretion experiment conducted between it and the current state-of-the-art (SoTA),

Chapter 4 breaks down the design of CASET and experimental validation of its working principles, and finally Chapter 5 summarizes the learned techniques from each project and the future work for each device.

Chapter 2

Design and Experimentation with Human-Interactive Robots

2.1 Review of Existing Haptic Devices

Haptic/kinesthetic robots have been around for many years, each using varying methodologies and designs to meet the requirements of those applications. This section reviews relevant literature and designs in the realm of haptics, with an emphasis on existing kinesthetic devices as well as other forms of human-interactive robots.

2.1.1 Types of Haptic Devices

Tactile Haptics is the realm of haptics that deals primarily with micro-scale touch effects, regardless of hand/finger position relative to the world. These responses are primarily felt through lower level mechanoreceptors responsible for sensing changes within a certain area [12]. By engaging these mechanoreceptors, different surface textures and geometries can be emulated. There are many different ways to create tactile haptics: pin arrays (which can be actuated using air, motors, microfluidics, etc.), electrostatics, vibration, thermal, and more.

Tactile haptics are increasingly popular in VR simulations due to its ability to simulate object feel for relatively low weight [13]. This allows many tactile haptic devices to be *ungrounded*, meaning they are donned by the user. Ungrounded devices have the benefits of an increased range of motion at the cost of force output, which falls in line with the primary use case of tactile haptics: simulating object texture, shape, and feel.

In contrast, **Kinesthetic Haptics** often comes in the form of *grounded* devices which are designed to produce macro-scale force vectors and trigger kinesthetic receptors to simulate

dynamic interactions with objects in an environment. Fig. 2.1 displays the differences between tactile and kinesthetic haptics with an example of a user holding a textured ball:

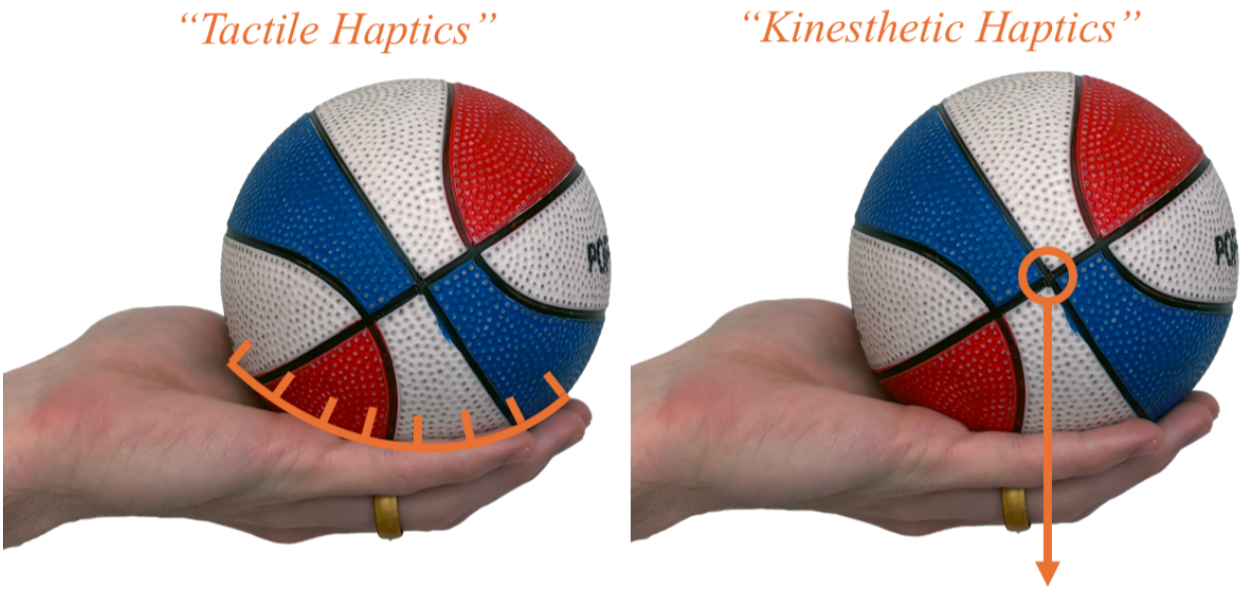

Figure 2.1: A user holding a textured ball, with the texture or inertia of the ball interacting with the user shown. The ball's inertia is best simulated virtually using kinesthetic haptics, whereas the texture and general 'feel' of the ball is best simulated using tactile haptics.

Kinesthetic devices are usually grounded as they require higher force output to mimic the inertia of real-world objects in haptic simulations. This often leads to a constrained workspace limited by the mechanical reach of the kinesthetic device. As one of the main devices in this manuscript, SER, is a kinesthetic device based on many existing robots such as the 3D Systems Touch and PHANToM Premium, subsection 2.1.2 will break down and cover a multitude of these robots.

Both tactile and kinesthetic haptics focus on human touch and mechanoreceptors interaction, but for the most immersive simulations, **Visual Haptics** are commonly integrated. Through a compilation of studies distilled by [14], the integration of VR in rehabilitation studies often creates higher success rate in navigation tasks. The same studies tested and used different haptic devices, such as haptic gloves, VR controllers with vibration, ankle-based robotic platforms, and more to improve immersion and interaction for (primarily) navigation tasks. Some of these devices leverage tactile haptics, some kinesthetic haptics,

and all involve the combination of these touch-based haptics with visual haptics through VR. Rose et al. concluded from these various studies that the 'right' haptic device for the situation is dependent on a multitude of factors, and improper device selection can actually harm user experience.

Virtual haptics can be the mimicking of real-world interactions in a virtual space to show objects that may not really exist, but it can also be used to generate pseudo-haptic effects by intentionally mismatching the user's avatar with their real-world orientation/state. In a study by [15], a completely passive device that leverages no kinesthetic or tactile haptic methods was used to simulate force feedback of a spring with visual effect alone. While participants of this experiment were able to discriminate between virtual and real springs, the visual effects generated an overestimation of the stiffness levels generated by the virtual spring.

Both Rose et al. and Lécuyer et al. show how visual haptics alone might not be powerful enough to trick users, but when combined with tactile and kinesthetic haptics can significantly impact their interpretation of virtual environments. Thus, when combined *properly*, kinesthetic haptics, tactile haptics, and visual haptics can create more immersive simulations that can 'fool' the brain [16]. Fig. 2.2 visualizes the implementation of all three haptic methodologies into an example simulation of a pill-placing task in VR.

2.1.2 Review of Existing Haptic/Assistive Devices

The new devices proposed in this thesis, SER and CASET, are both inspired by other kinesthetic and haptic devices. These devices, their working principles which may appear in SER or CASET, and why those principles were used are described in this section.

One of the most impactful kinesthetic robots is the PHANToM Premium pictured in Fig. 2.3 [17].

The PHANToM Premium is a 3 degree-of-freedom (DOF) kinesthetic robot designed to provide low-level force output to influence users that may interact with a stylus. The

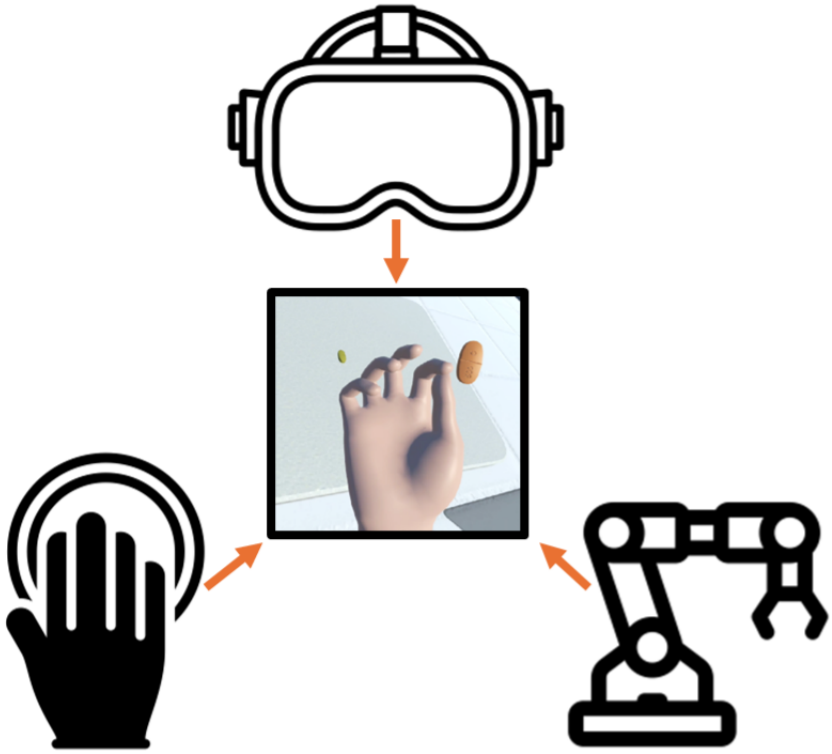

Figure 2.2: Kinesthetic, Tactile, and Visual Haptics can all be combined to create immersive simulations. Understanding the balance between these aspects and choosing the correct means for the simulation is crucial.

robot achieves 3-DOF movement through the use of three DC motors and capstan drives for each DOF. The yaw DOF is controlled by rotating the entire assembly which consists of a rotating four bar to create planar, 2-DOF, motion in the direction rotated by the base. The rotating four bar in particular is an extremely useful way to achieve the same range of motion (ROM) as a rotation-rotation arm whilst keeping the two driving motors closest to the origin, thus minimizing (or eliminating entirely) the moments generated by the weight of the motors.

Many PHANToM-based devices have been developed and released since the PHANToM's origin. One of the best examples of this is the 3D Systems Touch haptic device as seen in Fig. 2.4.

The 3D Systems Touch device utilizes capstans to get high torque out of high speed DC motors, but instead of a rotating four bar the devices uses belts and pulleys to achieve

Figure 2.3: The PHANToM Premium haptic device. This early kinesthetic robot provided the foundation for many capstan-driven, multi-DOF, force-feedback kinesthetic robots that came after it such as the 3D Systems Touch and SER.

3-DOF motion. This allows for a large ROM, but the devices is only able to achieve 3.3N of force output at the stylus endpoint. This is sufficient for many use cases, but as will be discussed in the SER section of this manuscript it is not sufficient to overcome the force output of a human finger.

A glove-based haptic device for object interaction is the G1 haptic glove system developed by HaptX [18]. The entire HaptX G1 system, with air pack, can be seen in Fig. 2.5.

These gloves use air powered microfluidics to produce both kinesthetic and tactile feedback through finger flexion locks and fingertip pin arrays. This technology was specifically designed for VR immersion, particularly for simulated training scenarios. Since the system was designed with an intended use case in mind, there are mechanical aspects of the design that fail to achieve certain haptic effects desired for the SER experiment described in chapter 3. More information pertaining to development with the HaptX system in the SER experiment is described in section 3.2.

Figure 2.4: The Touch haptic device produced by 3D Systems [1]. This PHANToM Premium inspired grounded kinesthetic robot is used in various haptics experiments and drawing/training programs.

While these devices are designed for low-force human interaction in haptics, humans may also interact with existing devices which are designed to provide assistance through force generation. Whether to provide more convenient means of movement for injured persons, or to extend the ceiling of human capabilities, human-assistive robots can come in many forms.

While most robots are designed with a specific use case in mind, they, or at least the working principles behind them, may be useful in other situations. A great example of this is the SPAR glove pictured in Fig. 2.6.

The SPAR glove was originally developed for assistance for users with activities of daily living (ADLs) by providing assistance to grip strength [2]. However, this device heavily inspired the development of CASET with its unique working principle of cable-driven trapezoidal links to produce a curling motion. In that case, a device's working principles become

Figure 2.5: The HaptX G1 haptic glove system.

Figure 2.6: The SeptaPose Assistive and Rehabilitative (SPAR) glove developed by Rose. This wearable device uses cables and 3D-printed links to provide grip assistance while using EMG to detect user intent.

adapted to a completely different situation. This level of inspiration in design is an important part of the feedback loop in modern robotics development.

From some of the foundational reviewed by [19], supernumerary limbs can be used in a multitude of the assistive tasks previously described. A great example of how a supernumerary limb may be used to increase human capability for otherwise inhibited users can be seen in Fig. 2.7.

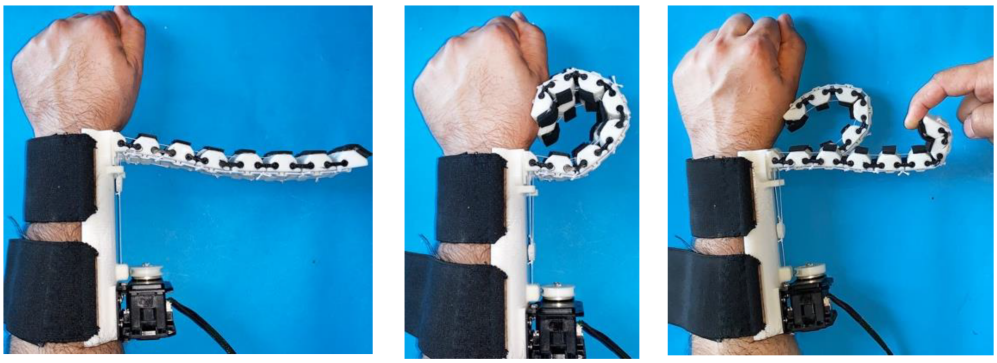

Figure 2.7: One of many 'sixth finger' assistive robots developed by [3]. Utilizing similar geometric principles as the SPAR glove and CASET, an assistive grip device can help stroke patients with difficult handling tasks.

These devices create additional interfaces for objects for when users (such as stroke patients) are either incapable of moving other fingers or desire an additional interface for smoother interaction. These principles could also be enhanced by an even greater increase in force output, which is one of the primary working principles behind some of the work in this manuscript (CASET).

Similar to the CASET project described in this manuscript in chapter 4, other supernumerary devices have been developed for litter carry assistance. A prevalent example of this is the device designed by [4], which uses springs and a back-mounted device anchoring shown in Fig. 2.8.

Other examples of assistance-focused devices and/or supernumerary fingers can be seen in the works of [20] and [21]. These assistive devices may be passive or active, but still rely on key mechatronics principles and, in many cases, cables to transmit the force. Multiple design characteristics from each of theses devices were used as inspiration in the development of both SER and CASET.

Figure 2.8: A supernumerary device developed by Liu et al. to offload litter carry, similar to the CASET device in this manuscript.

2.2 Review of Relevant Haptics Measures and Experiments

The types of haptic devices previously described: tactile and kinesthetic, deal with mechanoreceptors and kinesthetic receptors respectively [22].

Mechanoreceptors, as described by Johnson, are responsible for micro-level touch sensation on one's skin. In the context of haptics, the mechanoreceptors I am most concerned about are located in highly concentrated quantities in the fingertips and can be labeled as follows and described in Fig. 2.9:

- Meissner's Corpuscles – Detect light touch and 30-50Hz vibrations
- Merkel Cells – Detect consistent, steady pressure, shape, and deformation used for object identification
- Pacinian Corpuscles – Detect deep, sharp pressure and high frequency (250Hz+) vibrations
- Ruffini Endings – Detect skin stretch and consistent pressure often used in grip adjustment of the hand

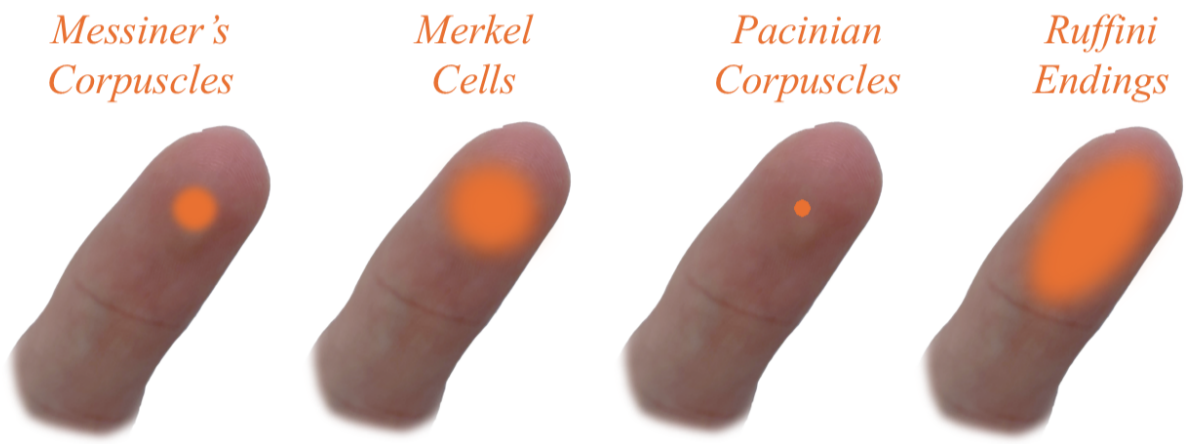

Figure 2.9: The four mechanoreceptors that deal with touch interactions and a visualization of their detection capabilities.

For macro-level tasks and joint-level sensing, one's body utilizes a multitude of kinesthetic receptors in a process known as kinesthesia [23]. These receptors are responsible for the knowledge of one's joints locations, with or without visualization of said joints. In kinesthetic haptics, the goal is often to either directly manipulate the joints or to trick the body's kinesthesia through a misleading pseudo-haptic effect. Most kinesthetic devices, including the devices described in the previous subsection 2.1.2, are designed with the intent of manipulating joint locations to trigger kinesthesia reactions.

Given the variance in potential kinesthetic robot designs, it's important to understand user preference and ability to discriminate between different devices.

An extremely popular metric to determine user detection thresholds and make control and device decisions for simulation is Just Noticeable Difference (JND) [24]. [25] observes that humans are not ideal observers and instead behave probabilistically. This idea has been reinforced by papers such as Stern and Johnson and unveils a sigmoidal trend line that appears in a multitude of psychophysical experiments, an example of such a plot can be seen in Fig. 2.10.

The reason Fig. 2.10 and other JND experiments appear as a sigmoid is due to the nature of stimuli detection. As you approach high stimulus, its inferred that you would achieve a near-100% discretion rate and vice versa for low stiffness and 0%.

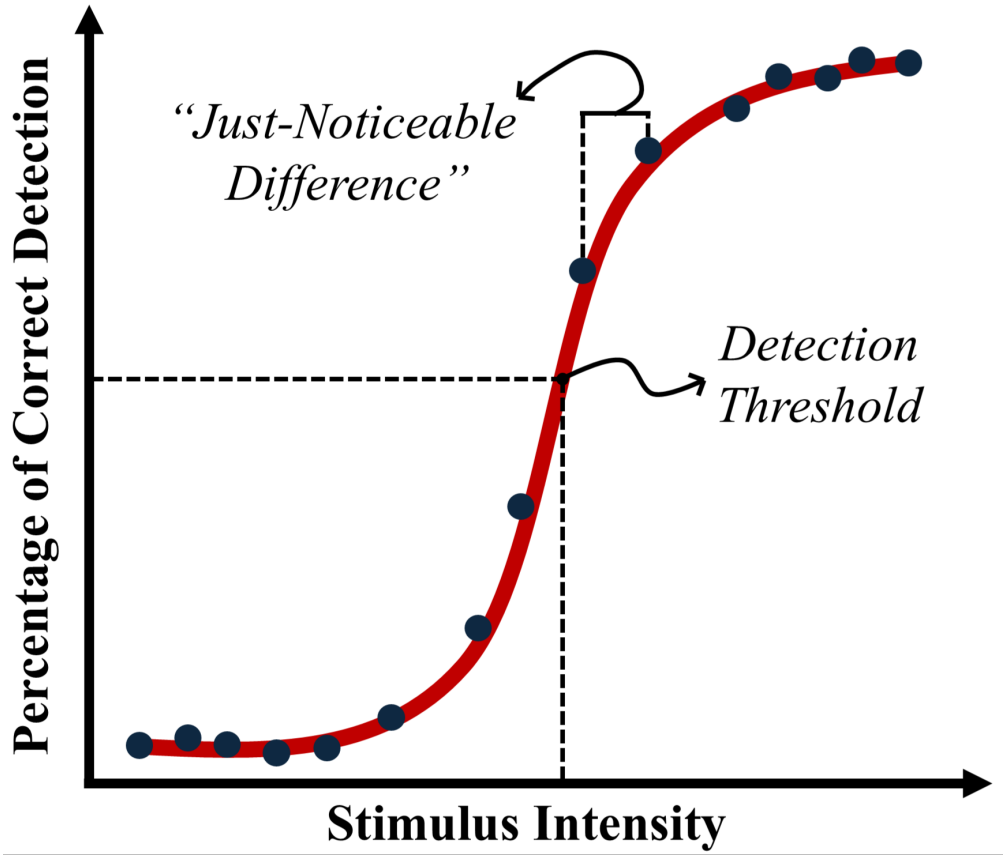

Figure 2.10: An idealized plot from a JND experiment. The trend line is shown in red and individual detection points from the experiment are shown in navy. The detection threshold is shown at about 50%, and the JND can be visualized as the change in stimuli between detection points.

A popular way to achieve JND results in haptics and psychophysics, such as those displayed in Fig. 2.10 is through the staircase method [26]. Once a subject detects a stimuli successfully the stimuli is lowered, and vice versa. This process is reapeated until a predefined number of "reversals" (switching from "yes" to "no" in back-to-back interactions) are triggered, and that stimuli point is defined as the subject's 50% detection threshold.

JND experiments are essential to understand detection thresholds for ranges of stimuli, such as the amount of impedance generated by a kinesthetic device. This information allows for a better understanding of how to control haptic devices to a degree which is detectable by the average user.

While many robots are created to improve haptic interactions and create specific sensations in virtual simulations, assistive robots may have other measurable metrics to validate their usefulness. For load-bearing assistive robots, such as developments like [27], the primary objective is to change the distribution of load on a wearer from smaller/weaker muscle groups to larger/stronger ones to reduce fatigue. By translating loads through robotics, I can reduce fatigue and improve human performance for various tasks, such as maintained control of a system or increased carry-time.

2.3 Cables and Capstans - When and Why?

Designing robots for human interaction requires quick, direct feedback and load transfer over long distances. Cables provide an exemplary way to transfer or increase loads in these mechanical applications. Through capstans, cables provide a no-backlash alternative to gear reductions, producing high torque output from high-speed DC motors [28]. With the use of Bowden cables, tension can be translated over long distances with nearly unlimited directionality [29].

Capstan drives are an increasingly popular way to achieve no backlash in gear reductions often necessary to get higher torques out of human-interactive robots. The basics of a capstan can be seen in Fig. 2.11.

However, capstans are not without their own challenges. The primary issue with capstans is a matter of tension. Over time, cables stretch, and when cables stretch the capstan system becomes highly nonlinear and unreliable. To fix this, capstan drives are usually tensioned actively or passively. An example of an actively tensioned system is the tensioning system developed by [30] for a tendon-driven surgery kinesthetic robot. An example of a passive system would be the screw-in tensioners used for SER (described in section 3.3), visualized as gray screws in Fig. 2.11.

Also, by introducing a friction component to the system with the capstan drum and cable, one can introduce nonlinearities that impact the effectiveness of used control methods.

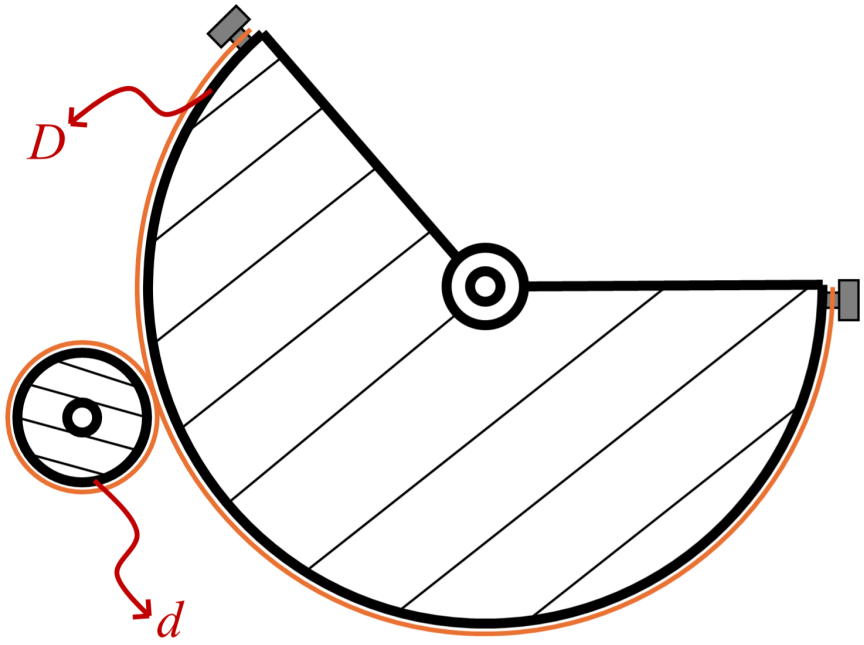

Figure 2.11: A visualization of the working principles of a capstan drive. The ratio of the driving and driven disks, d and D respectively, is what creates the gear reduction.

To minimize these effects it is essential to maximize the friction coefficient between the cable and drum (often by changing surface effects or material) and ensure that the drum radius is greater or equal to the minimum bend radius of the cable being used. By ensuring these things and maintaining proper tension on the cable of the capstans, one can achieve near-ideal feedback on high gear reduction applications.

For assistive robots, there is often a need to translate forces over great cartesian distances, not just to increase rotational torque output. To achieve such an effect, Bowden cables provide a 'guide' for the tension-carrying cable through the desired path and over the desired distance which can be seen in Fig. 2.12.

The torque transfer from Bowden cables is near-instant, barring the elasticity of the cable used.However, it's worth noting that Bowden cables often suffer significant losses due to friction which can be mitigated by straightening the travel path and increasing the rigidity to prevent crumpling. As the tension T increases, the Bowden cable itself begins to 'harden'

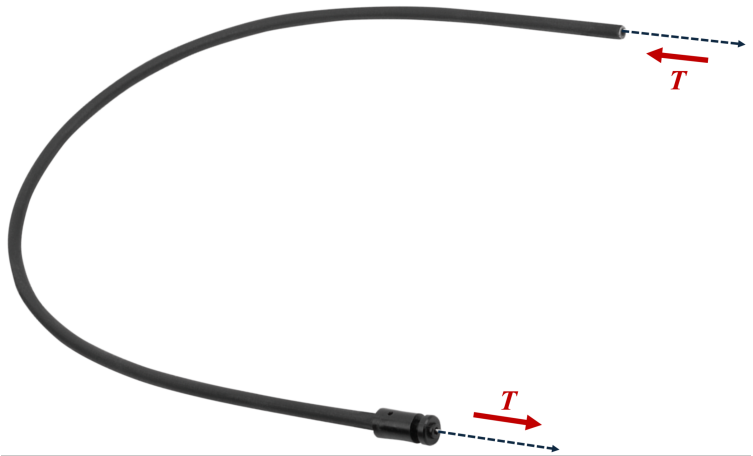

Figure 2.12: How a bowden cable transfers tension T over an arbitrary path.

into the shape that it was in before tensioning. This reduced the effectiveness of polymer-based Bowden cables, and provides the basis for the development of metallic Bowden cables such as Jagwire, which was used in the development of CASET [31]. The addition of metal links to Bowden cables helps reduce the crumpling effect under tension, but in practice these cables are still stiffer and retain their shape under load.

In both uses of bowden cables and capstans for SER and CASET in this manuscript, various steel cables were used to minimize stretch and reduce the need for constant tension adjustment.

2.4 Additive Manufacturing in Robot Design

Additive manufacturing (AM) is the process of generating a product through a layer-by-layer approach instead of machining down existing material into the desired shape [32]. Additive manufacturing has been a quickly growing industry as the increase in part turnaround is significant especially in robotics and rapid prototyping situations. However, utilizing AM properly for these experiments required some testing and quick experimentation to distill the most effective parts for the SER and CASET projects.

The adjustable parameters in Table 2.1 are what effect the strength, directionality, and quality of a printed part. Since the modification of these parameters offers hundreds of valid,

Table 2.1: Adjustable parameters in the average 3D-Print.

Parameter	Description
Perimeters	Strength - The greater number of perimeter loops around the part and its openings, the greater the strength of the part
Infill	Directionality - Infill type and print direction change the nonlinear, anisotropic properties of a print
Layer Height	Quality - Smaller layer height produces higher quality prints with the increased resolution of more layers

printable parts, it's important to have a general understanding of realistic desired parameters for the part in question.

In most engineering applications, print quality is not high priority as modeled parts for robots are usually relatively simple geometrically (as opposed to organic models). Therefore layer height (which ranges from 0.05mm to 0.35mm for most printers) for most parts in this manuscript is set to 0.15mm, with many quick turnaround parts in the prototyping phase printed at 0.3mm.

2.5 Sensors, Motors, and Other Electronics

To achieve desired dynamics for electromechanical systems, the most common method is the use of Direct Current (DC) Motors. DC Motors work by converting electrical energy into mechanical motion through electromagnetic interactions and can be controlled through voltage or current inputs [33]. There are two types of DC motors: brushed and brushless, where brushed use a rotating commutator that physically touched individual 'brushes' to create electromagnetic field and brushless are commutated programatically (thus requiring more complex controllers). Fig. 2.13 displays the two DC motors used in this manuscript's experiment.

DC motors are generally designed for high speed, low torque output. Therefore, to achieve high torque applications (which are often desired for humans who move relatively slowly but generate high forces) methods like gear reductions or capstans are required. While

Figure 2.13: The (left) Maxon 20W RE25 [5] and (right) Pololu 8.4W with 75:1 gearbox [6] DC motors used in SER and CASET respectively. In this case, the higher cost of the Maxon motor results in better efficiency and responsiveness, and access to Maxon's own 4096 CPR encoders. For CASET, a cheaper motor with a build in gearbox and less accurate encoder was desired.

SER utilizes the previously described capstan, the DC Motor in Fig. 2.13 has an attached sun gear driven assembly to create a 75:1 ratio.

To control brushed DC motors, a motor controller that converts voltage to current output is often used since most off-the-shelf micro-controllers can easily generate analog voltage outputs. The motor controllers used by CASET and SER are shown in Fig. 2.14. Similar to the DC motors for these projects, higher cost in motor controller results in more accurate control, higher power output, and more flexibility for use with various DC motors.

Figure 2.14: The (left) AMC CB12A1C [7] and (right) Pololu DRV8874 DC motor [8] drivers used in SER and CASET respectively.

To accurately control robotic systems and implement feedback, proper sensing of joint angles to calculate cartesian positions is necessary. To do this, rotary encoders are often used. Rotary encoders work as seen in Fig. 2.15 by passing a laser through gates in a wheel and

counting the number of times the laser has passed through [34]. Higher count-per-rotation (CPR) encoders are higher quality due to capturing more information per rotation.

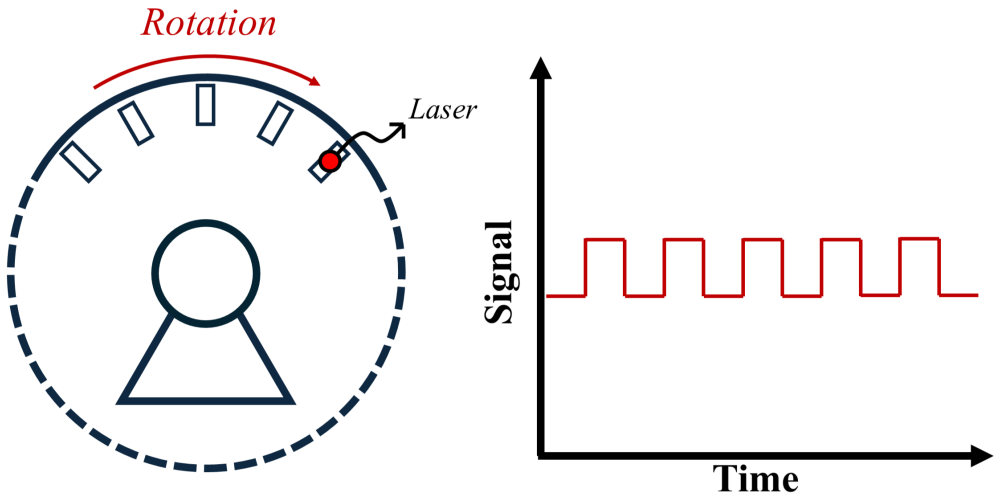

Figure 2.15: A rotary encoder works by rotating a disk containing slits and having a laser pass through each slit, sending signal while it does. The frequency and size of signal pulses can be used to determine rotation speed.

2.6 Programming and Controls of Robotic Systems

Robotic systems, both in rehabilitation and assistance, are useless without sufficient means of control. To complete a task, a robot must not only have the means of achieving a performance, but a program telling it how and when to achieve said means.

The most primitive form of control is on/off control [**?**]. By relying on a single condition to determine if the device should be on at full capacity or completely disabled, one can sometimes sufficiently control systems that are either extremely simple or highly resistant to change. The basic process of an on/off controller is displayed in Fig. 2.16 using an A/C unit of a room as an example.

However, in many cases the binary action of an on/off controller is insufficient. In these situations, classical control methodologies may be used. By distilling the measurable states of a system to their most basic components, like the position of an inverted pendulum, one

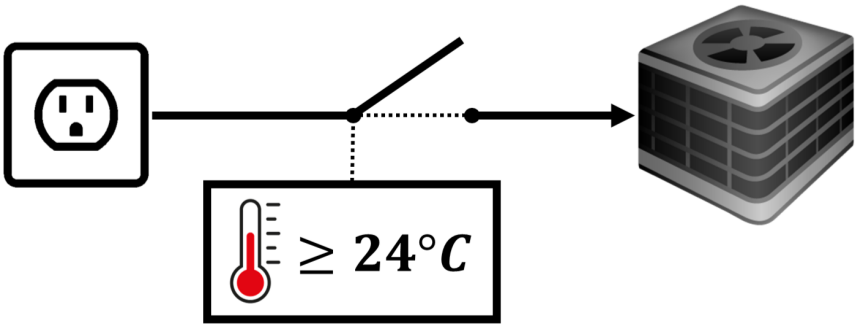

Figure 2.16: How a hypothetical on/off controller may make control decisions.

can make informed decisions on how to modify these states to achieve another set of desired states as described by **?** .

In robotic systems, we often have the ability to track the location of the system through position measurement devices like the encoders described in 2.5. By applying classical control methods to these measured positions in order to achieve a desired trajectory or position, 'position control' is implemented. To achieve a desired response to this control can be adjusted not only proportional to the desired position, but also to the change in that position, or velocity[35]. This description of a simple PD controller is displayed with the following equation:

$$\tau = K_p \cdot e + K_d \cdot \dot{e} \tag{2.1}$$

Where K_p and K_d are the respective control gains based on the measured error of the position-states, e and $\dot{e}$, derived from:

$$e = \theta_{\text{desired}} - \theta_{\text{actual}} \tag{2.2}$$

In this simplified system, the controlled output is an arbitrary force that would, when selecting appropriate values for K_p and K_d, minimize the error e.

However, the robotic systems discussed in this paper interact with humans and objects in the real world, so simply attempting to minimize the error to a desired trajectory is

insufficient. To control the device in a manner that sufficiently incorporates both the robot and the environment around them, a modify version of PD control called "impedance control" may be used [36].

Impedance control is extremely similar to PD control in that the main objective is still to minimize error, but instead of treating the robot like it exists in a vacuum, one may incorporate the knowledge of interaction forces from the environment into the control. Table 2.2 depicts the conceptual differences between PD and impedance control.

Table 2.2: The difference between PD and Impedance control.

Feature	PD Control	Impedance Control
Goal	Track position/velocity	Regulate force/motion interaction
Behavior	Stiff (high gains)	Compliant (gains inc. force)
Best for	Free-space motion	Interaction tasks
Controls forces?	Indirectly	Directly

While PD controllers *do* control force indirectly through position error, they do not directly capture force interactions. This can make it very difficult to get the real-world desired interaction with a robotic system using PD, as the conversion from positions to forces is not straightforward. Impedance control introduces a mathematical way to fix this. From Hogan, there exists a force-position relationship that can be applied to the robotic system:

$$F = M(\ddot{x}_d - \ddot{x}) + D(\dot{x}_d - \dot{x}) + K(x_d - x) \tag{2.3}$$

Where the desired/actual states of the system, x_d and x, are the desired/actual endpoint position of the robot which must be derived from a series of known joint relationships [37]. In this case, the gains, M, D, and K, are intended to act as a mass, damper, and spring effect for the end effector.

By using impedance control, one effectively treats the device's endpoint as a single point in free space that have complete control over the dynamics of. Through the control of this point, one can interact with the environment however necessary.

Chapter 3

SER - The Stiffness Emulation Robot

Rendering internal impedances is key for developing immersive experiences in virtual reality (VR). While previous research has primarily focused on the rendering of external impedances, rendering changes to the avatar remains an open question. Changes to the avatar are particularly salient for disease education and fostering empathy in healthcare professionals in conditions such as Rheumatoid Arthritis (RA). As a first step towards this immersive experience, this study explores whether humans can distinguish between joint and endpoint impedances. I developed a novel robotic system (Stiffness Emulation Robot) and a new controller for an existing haptics glove (HaptX G1), and conducted a binary discretion experiment which reveals that the majority of subjects can differentiate the two impedance types.

3.1 Background - Why Build a Stiffness Emulation Robot?

Combining haptic interfaces with virtual reality (VR) systems has been the focus of years of successful research and commercial activity to develop devices and methods for rendering the sensations of interactions between a virtual avatar and their virtual environment [14]. Typically, the avatar is able bodied, or at most, as able as the wearer by default. However, there are several applications where convincingly and clearly rendering a virtual avatar with diminished capabilities could convey crucial system limitations to the operator. Notably, individuals with progressive, chronic diseases could experience limitations in motor function that could arise if preventative interventions are not followed [38].

Despite this need, there have been few investigations into methods to enable the embodiment of such internal or structural differences between the operator and the avatar. There

are open questions on how to convincingly simulate such differently abled bodies, in terms of changes not to just their structure or perception (height, color vision) but also internal, biomechanical changes (joint number, stiffness, or strength). The creation of this sensation is particularly challenging, as it requires first understanding, and then changing the perception of mechanics internal to the user, and not the external or environmental dynamics which have been previously studied.

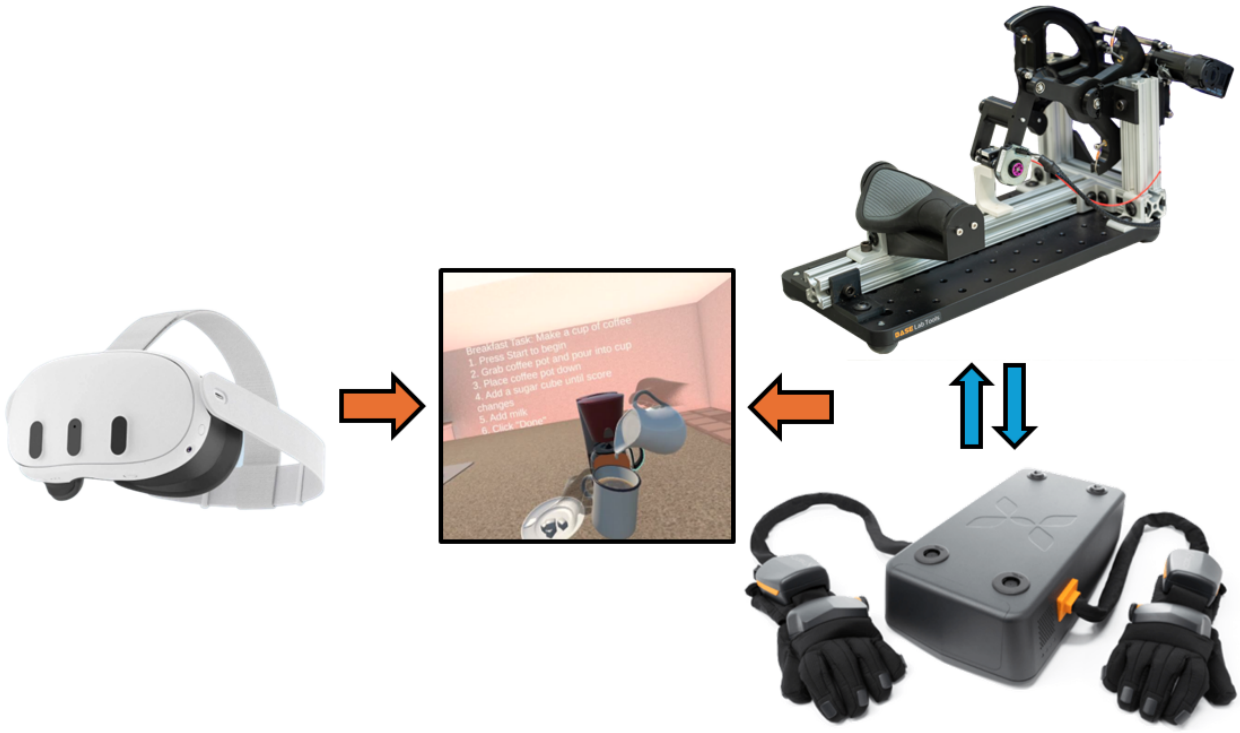

Figure 3.1: The current state-of-the-art in haptics is not designed with internal changes to avatar in mind. To fix this problem, this study will quantify people's ability to perceive different representations of internal mechanics (joint or endpoint impedances) rendered by the HaptX G1 and Stiffness Emulation Robot (SER) respectively.

As an application, progressive diseases such as rheumatoid arthritis (RA) are an appealing case study as they both have a need for communicating these internal changes, and also have the experience of these internal changes. Communicating and more importantly, understanding the consequences of disease progression with or without pharmacological interventions is an open challenge, and an obstacle towards improving medical outcomes. For both the clinicians and patients, it is difficult to weigh the adverse effects of medication now

with symptoms in the future which have yet to be experienced. If clinicians are able to experience RA in a meaningful and clear way, they may have increased empathy and ability to help their patients make difficult decisions [39]. Similarly, if patients could experience potential future outcomes, they may be able to make more informed and balanced choices at earlier stages of this progressive disease. This approach of episodic future thinking in patients has demonstrated efficacy in reducing temporal discounting, influencing health behaviors, and increasing empathy but requires that individuals possess accurate information about future experiences [40].

Our hypothesis is that while the perception of endpoint and joint level impedance can be perceived, there are pseudo-haptic approaches that can close this gap [41]. Before exploring these different approaches as seen in Fig. 3.1, I must first confirm this hypothesis and see if humans can perceive different impedances, which is the primary objective of this paper. Sections 3.2 and 3.3 introduces the Stiffness Emulation Robot (SER) and the HaptX G1, including a breakdown of the new, pulse-width modulation (PWM) control of the HaptX G1 finger locks, and the experimental protocol for a ten participant experiment. Section 3.4 covers the results of the binary discretion experiment, where participants reported which stiffness type they were experiencing on their index finger. Section 3.4 also discusses how this experiment's results show that humans *can* detect a difference between joint and endpoint impedance, and how other experiments could provide more information to improve internal actor mechanics for future VR simulations.

3.2 The Current State-of-the-Art: HaptX G1

HaptX is a company that has been focusing on developing a unique haptic device for virtual object emulation. This device, the HaptX G1, is described in the following subsections as an example of the current state-of-the-art in haptics technology.

3.2.1 HaptX G1 Working Principles

The HaptX G1 is a haptic glove designed for VR immersion enhancement. The device uses air powered microfluidic tactile actuators and finger locks to provide realistic feel and force feedback in VR environments. To invoke an impedance on the G1 wearer's finger, the finger locking mechanism (capable of 8 lbs force output) was controlled via PWM, a novel implementation on this particular device. The HaptX system runs at a maximum of 120 Hz, but due to mechanical limitations of the solenoids that actuate the finger locking mechanism, the fastest achievable PWM period of the finger lock was discovered to be 30 Hz. The best tested operating PWM duty cycle at 30 Hz was 15%, with actuation percentages much higher or lower resulting in either no actuation or complete lockup, respectively. In cases where human movement is being analyzed, PWM frequency must be sufficient to capture human sensing and movement capabilities.

Figure 3.2: A single HaptX G1 glove. The gloves come in four different sizes, and all work off the same HaptX air pack system to provide tactile feedback at the fingertips and force feedback to finger flexion.

3.2.2 Mechanical And Programmatic Limitations of the HaptX G1

The HaptX G1 was not intended to create levels of impedance less than the binary 8 lbs lock provides. This means that the PWM control is a way to manipulate the device, and therefore can only produce low levels of impedance. Through an experiment with the HaptX, SER, and a passive human hand (shown in Fig. 3.3), it was found that a single finger of the HaptX glove could produce impedance of about 0.0160 N/mm at a 30 Hz PWM period and 15% duty cycle.

3.3 Design and Working Principles of SER

SER is the product of multiple years of version iteration and design improvements. Borrowing traditional kinesthetic robot design concepts and implementing them in novel ways has resulted in a high force output 2 DOF robot capable of overcoming the force output of an index finger.

3.3.1 Version History and Improvements

SER initially began as a handheld kinesthetic device as seen in Fig. 3.4. As an ungrounded device, this version would have created unnecessary fatigue in a user who may be holding the device for the experiment without any real gain by being ungrounded.

SER V0 was never developed, but was used to visualize the rotating four bar geometry and capstan setup with heavily 3D-printed geometry. The first built version of SER was SER V1, seen in Fig. 3.5.

SER V1 was constructed in Fall of 2023, and while un-powered, displayed how the device would work geometrically. While the capstans were large to create a 14:1 ratio, the four bar geometry was relatively small, creating interference and significantly limiting the range of motion of the device. Also, the four bar geometry was all in a 'stack' where different bars were cantilevered off each other and there were too many parts to create the desired motion.

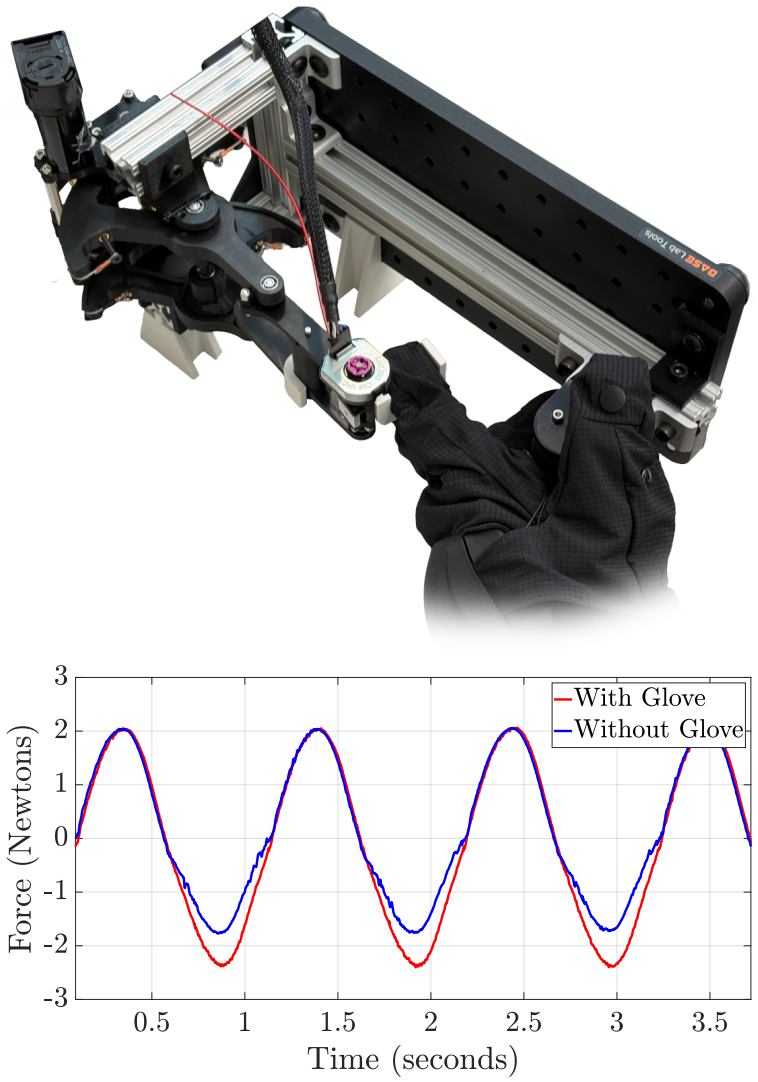

Figure 3.3: (Top) The HaptX G1 interacting with SER in the force output comparison test. The applied force at the end effector was measured with a load cell to determine the force rendered by the hand and glove. (Bottom) Quantification of the HaptX G1's force output. The blue segment shows the applied force by the passive hand with the HaptX disabled, and the red segment shows applied force by the same hand with the HaptX enabled at a PWM period of 30 Hz and a 15% duty cycle. The resultant force application over the translation distance for the HaptX G1 is 0.016 N/mm.

The prints for this version were done on an older, unmaintained printer which produced low quality parts that took too long to print. This was resolved by upgrading to Prusa Mk4 printers [42].

The follow up version of SER, V2, was developed with the intent of presenting some validation results at the International Symposium of Medical Robotics in June of 2024. This

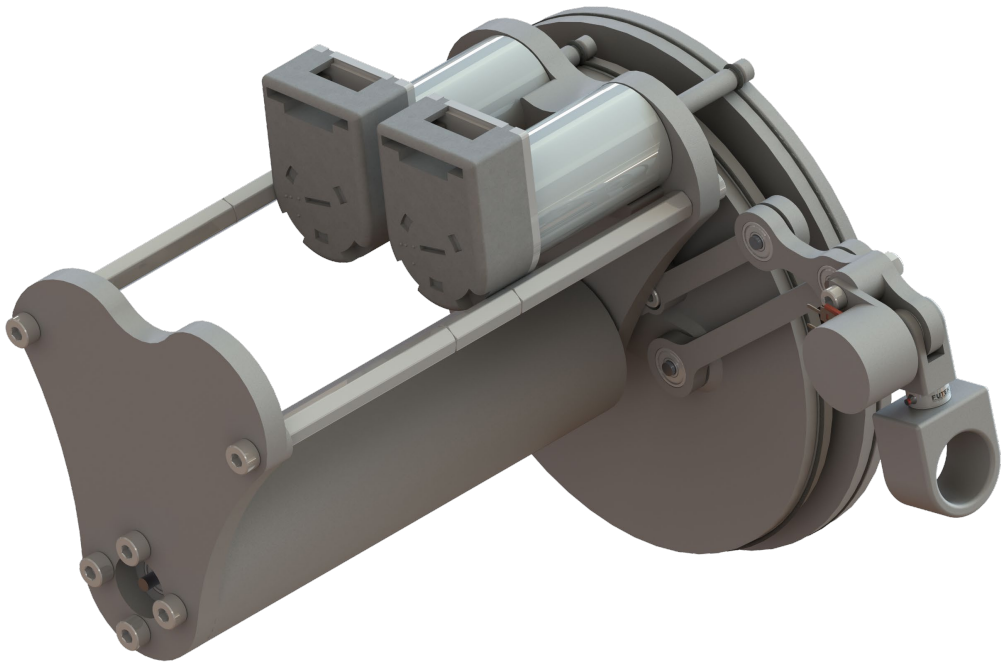

Figure 3.4: The original SER concept (Version 0.0). This model is ungrounded, which would cause unnecessary fatigue on a participant who might hold the device. The basic working principles, however, can all still be seen.

version would need a working PD controller to demonstrate the device's ability to generate stiffness, and can be seen in Fig. 3.6.

As this was the first powered version of SER, all of the electronic components were set up including the Quanser Q8, all motors and motor controllers, and all sensors and wiring. While both capstans included routed cables, all testing for SER V2 was only conducted with the capstan primarily used for creating up-down motion for simplicity.

The four bar links of SER V2 may share similar geometry to V1 when viewed at the side, but efforts were taken to eliminate cantilevered shafts wherever possible, which increased stability. Still, range of motion was impacted by these new complex parts that included segments that stuck out and interfered with the actuation of the four bar itself. Also, the capstans were too narrow for SER to reach its full ROM, and a failed capstan design that was V-shaped caused the steel cables to rub together, creating substantial friction.

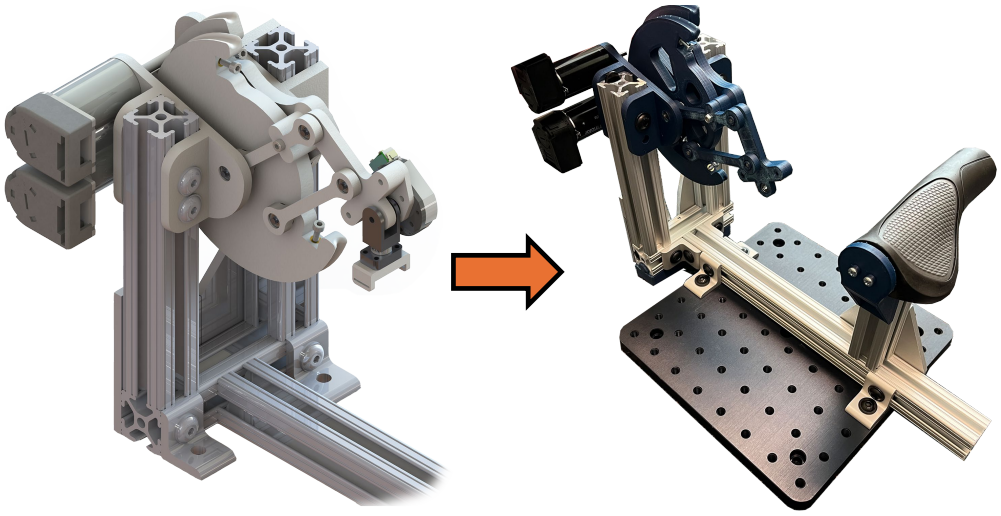

Figure 3.5: SER Version 1.0 in CAD and the first built prototype. Building the prototype highlighted interference and print quality issues which hindered range of motion, so this prototype was never powered.

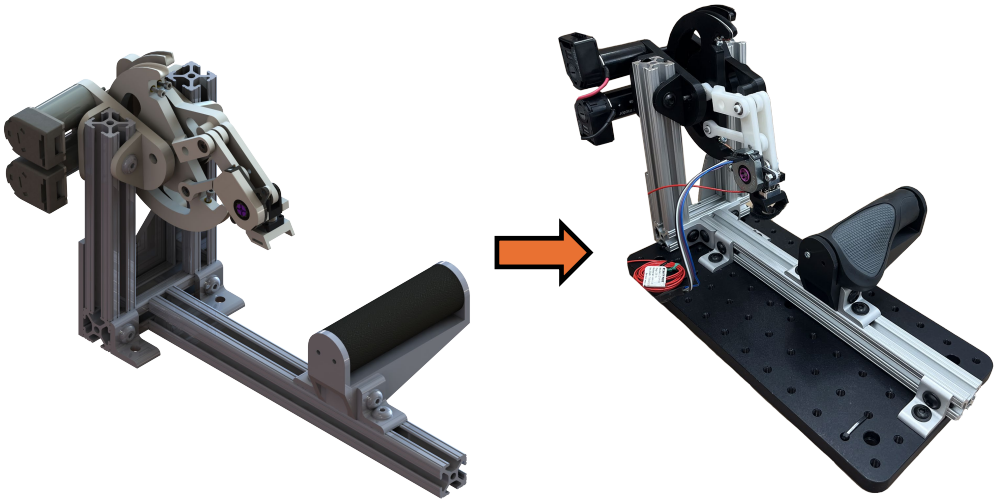

Figure 3.6: SER Version 2.0 in CAD and reality, the first powered prototype of SER. SER V2 was controlled using a simple proportional-derivative controller for a basic experiment to test feedback and load cell measurements.

After presenting SER V2, major revisions were in order to increase the range of motion, reduce complexity, and improve performance. All of these changes resulted in the development of the final version of SER, V3, seen in Fig. 3.7.

SER V3 was a complete from-the-ground-up redesign. By spreading out the entire rotating four bar between two upright segments of 8020, this version is far more laterally

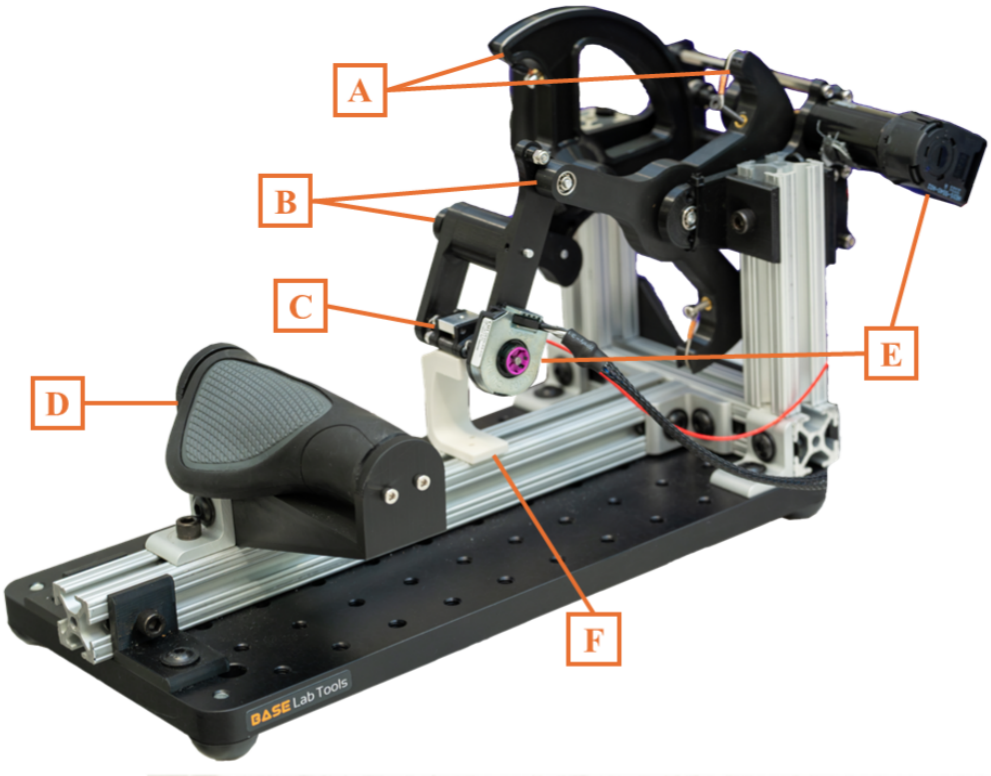

Figure 3.7: SER: The Stiffness Emulation Robot. Components labeled in the image are described in the table below.

Label	Description
A	Two-capstan driven system
B	Rotating four-bar mechanism
C	Free-spinning joint with load cell
D	Adjustable palm rest for subject's hand
E	Encoders for measuring each degree of freedom
F	C-clip interface for HaptX G1 fingertip

stable the V2 ever was, and each part was simplified geometrically along with the entire assembly, netting in the entire four bar being exactly four printed parts. Another benefit to spreading out the entire assembly, seen in Fig. 3.8, was a significant improvement in the device's ROM. The entire transmission was reworked to included doubly-supported shafts, and the capstans were all widened and flattened to improve min/max rotation and reduce friction significantly. A more detailed breakdown of the components in SER V3 can be seen in the following subsection:

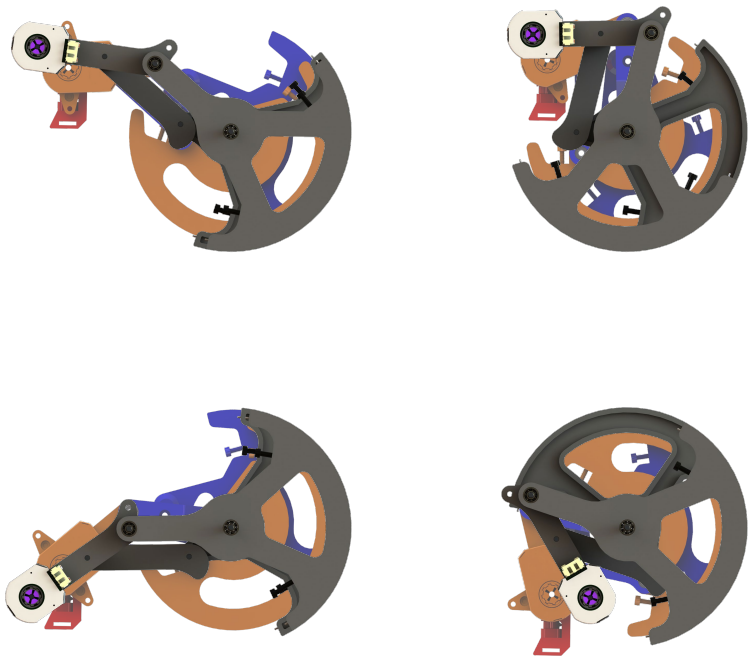

Figure 3.8: The range of motion improvements from SER version 2.0 (colored) to version 3.0 (grayscale). The real-world difference is even more substantial.

3.3.2 Working Principles

SER utilizes a multitude of kinesthetic device principles described in chapter 2 while modifying aspects of these principles to achieve the desired response.

SER's capstans were designed with the intent to match or overcome the average human index finger. Therefore, each capstan is driven by a 20W Maxon RE25 Brushed DC Motor and a 14:1 ratio resulting in 420 mNm of continuous torque per disk. Using these values, SER can produce a maximum of 76N of force in the vertical, "Y", direction and 38N of force in the horizontal, "X", direction at the endpoint of the rotating four bar in base configuration.

The end effector of SER contains a FUTEK 25lbs miniature in-line load cell (Part no. FSH04400) which records force output from the free-spinning endpoint. The load cell is sandwiched between two 6061 aluminum plates, machined so that the load cell is not interfacing with the relatively compliant PLA. The need for a free spinning endpoint comes from the nature of kinesthetic devices and the avoidance of over-constraint. Similar to devices like the 3D Systems Touch, a free spinning end effector allows for free movement of the user

who may be interacting with the kinesthetic device. This avoids any unnecessary discomfort or pain.

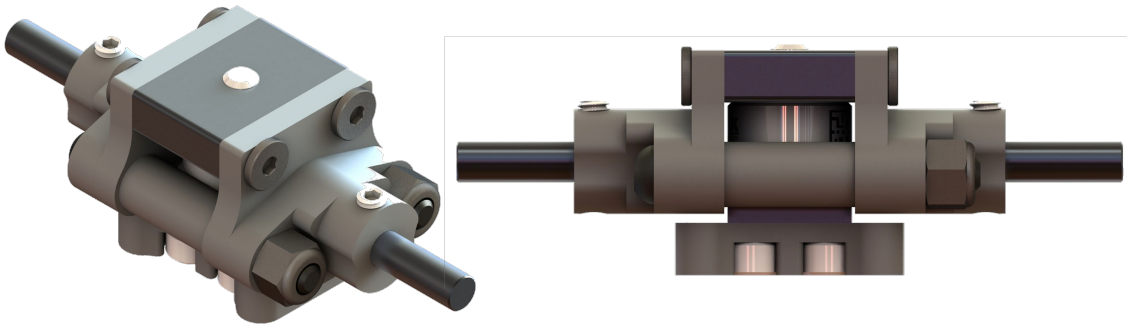

Figure 3.9: SER's end effector. This design utilized 3D-printed segments that interface with two machined aluminum 6061 plates located above and below the load cell. These provide a non-deformable interface with the load cell for accurate force measurement.

SER's transmission has changed drastically through interactions. Originally, the cantilevered shafts would bend and fail to hold the capstan cables. To fix this, the ends of the shafts *were* supported, but the actual capstan drums were press-fit between the motors and shafts. The drums themselves were also being used to connect the motor shafts to the aluminum shaft which was not perfect and thus bent very easily. Plus, the drums were too small to fulfill the minimum bend radius of the wire used which generated friction. The final transmission, seen in Fig. 3.10, aimed to fix all these issues.

First, by shifting to a machined shaft collar to connect the shafts and moving the drums to be contained within one shaft alone, the bending caused by those connections reduced. A third, intermediate bearing wall was also added to support both ends of each shafts, and set screws were added to the printed drums, allowing for them to be secured to the shaft without press-fitting. All of these improvements helped reduce assembly time, improved stability, and significantly reduced friction and breaking.

Other working principles are described throughout this manuscript, in background and experimentation.

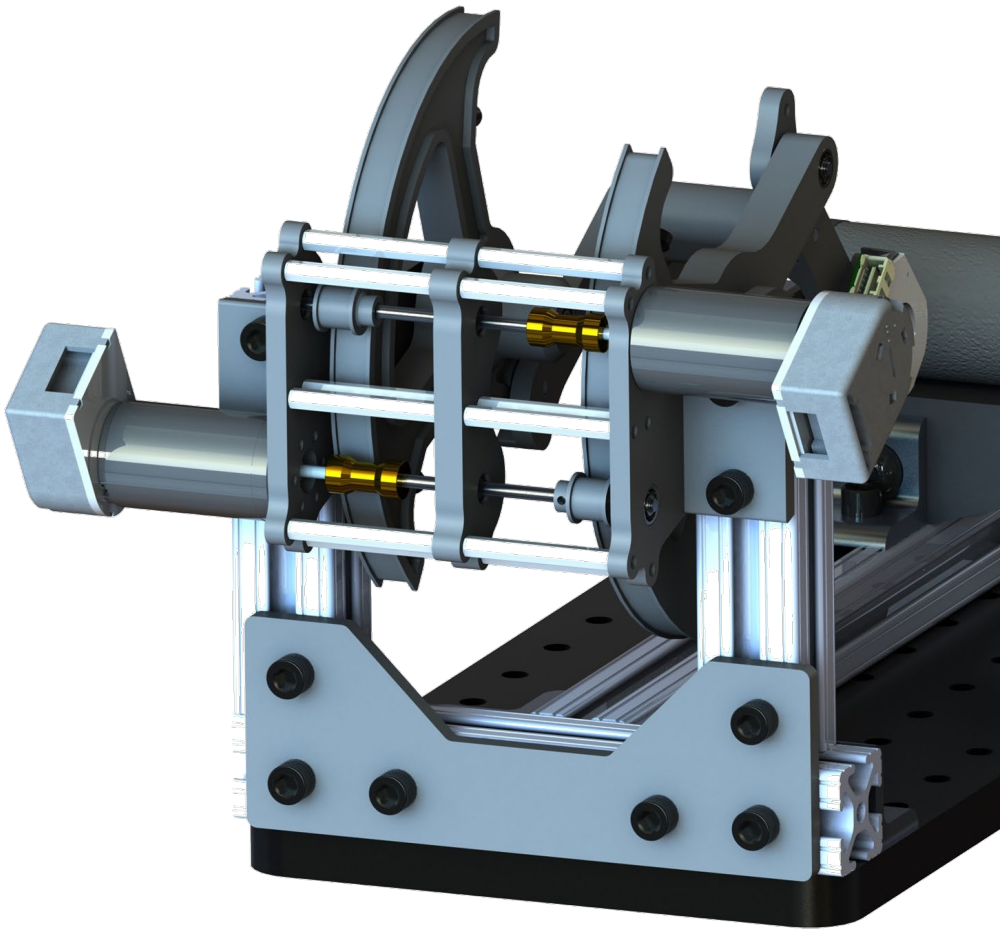

Figure 3.10: The 'transmission' used to deliver power from each motor to its respective capstan. Each shaft is supported twice each to improve stability significantly over previous cantilevered versions.

3.3.3 Controls and Implementation

To control SER, it is crucial to understand the kinematics and dynamics of the robotic system. As the rotating four bar of SER can be simplified to a simple rotation-rotation robot since it is parallel [43], SER's kinematics can be displayed as seen in Fig. 3.11.

To conduct the binary discretion experiment between SER and the HaptX, a simple controller to mimic the impedance created by the HaptX was used to control SER. Since the HaptX produces a damping effect with it's PWM control, SER ran on a derivative-only controller for the experiment. The following equations describe the D-controller used:

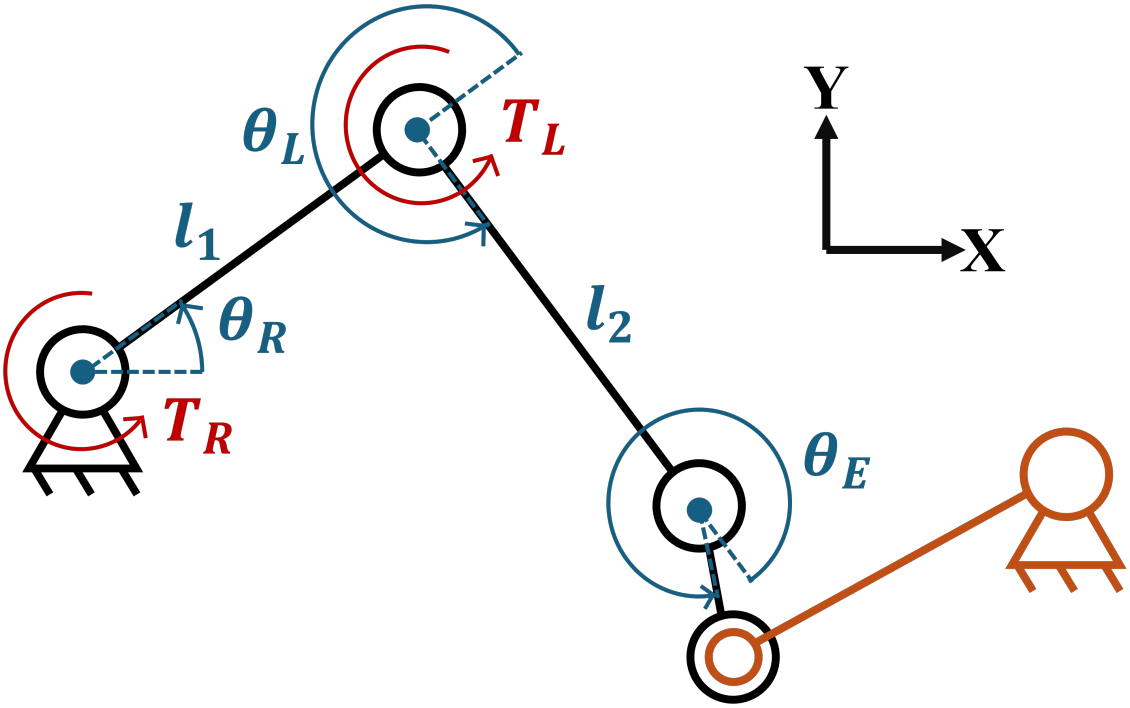

Figure 3.11: Simplified SER kinematic chain. The angles measured by each encoder, θ_R, θ_L, and θ_E, lengths of each segment, l_1 and l_2, and torques controlling each four bar link, τ_R and τ_L, are labeled, with the user's index finger shown in orange.

$$\tau_R = -\dot{\theta}_R \cdot K_D \tag{3.1}$$

$$\tau_L = -\dot{\theta}_L \cdot \frac{K_D}{2} \tag{3.2}$$

Where:

- $\dot{\theta}_R$ and $\dot{\theta}_L$ are the measured disk velocities
- K_D is the derivative control gain, the left gain being halved to mimic the 60mm to 30mm four bar ratio between the right and left disks.

While this controller most closely mimics the feeling generated by the HaptX gloves, further modifications were made to lower the fidelity and smoothness of SER as described in subsection 3.3.4.

For future experiments, a more effective way to control SER is through the use of a Jacobian matrix to turn the measured joint torques into endpoint forces [44]. The same kinematic chain shown in Fig. 3.11 can be used to derive a Jacobian.

To calculate the system Jacobian, the measured joint angles of SER must be converted to endpoint positions in the XY plane defined in Fig. 3.11 as seen in the following equations:

$$X = l_1 \cos\theta_R + l_2 \cos(\theta_R + \theta_L) \tag{3.3}$$

$$Y = l_1 \sin\theta_R + l_2 \sin(\theta_R + \theta_L) \tag{3.4}$$

As per [44], the Jacobian matrix for a two DOF/two measurement robot such as SER is a 2x2 matrix consisting of partial derivatives of Eqs. 3.3 and 3.4 with respect to the measured angles θ_R and θ_L as seen below:

$$J = \begin{bmatrix} \frac{\partial X}{\partial \theta_R} & \frac{\partial X}{\partial \theta_L} \\ \frac{\partial Y}{\partial \theta_R} & \frac{\partial Y}{\partial \theta_L} \end{bmatrix} \tag{3.5}$$

Taking these partial derivatives produces the following Jacobian matrix:

$$J = \begin{bmatrix} \frac{\cos(\theta_L+\theta_R)}{l_1 \sin(\theta_L)} & -\frac{l_2 \cos(\theta_L+\theta_R)+l_1 \cos(\theta_R)}{l_1 l_2 \sin(\theta_L)} \\ \\ \frac{\sin(\theta_L+\theta_R)}{l_1 \sin(\theta_L)} & -\frac{l_2 \sin(\theta_L+\theta_R)+l_1 \sin(\theta_R)}{l_1 l_2 \sin(\theta_L)} \end{bmatrix} \tag{3.6}$$

By taking the transpose of this Jacobian matrix, I can convert all known joint torques to endpoint forces in both the X and Y directions using the following equation:

$$\tau = J^T F \tag{3.7}$$

Future experiments that require endpoint control of SER may use this derived Jacobian, but it must also be understood that, by design, this does not control the free-spinning 3rd DOF connected to the endpoint of SER.

Figure 3.12: Input/output flow with the Quanser Q8 system and all SER components. Encoders and the load cell provide all inputs and the Q8 running SIMULINK produces voltage outputs to the DC motor controllers.

3.3.4 Combining with the HaptX G1 for a Comparison Experiment

To match the previously described hypothesis, the only factor that can impact participant decision-making was which impedance type they felt acting on their index finger. Various modifications to the experiment were made to reduce confounding factors. First, the binary discretion experiment was conducted with a finger splint placed over the subject's index finger. This prevents movement of the proximal interphalangeal and distal interphalangeal finger joints, meaning the only joint analyzed in the experiment is the metacarpalphalangeal (MCP) joint. Since the user may only move their finger at the MCP, the Cartesian impedance created by SER is actually a 'joint' impedance. This joint impedance is inherently different from the endpoint impedance previously described in subsection 2.2, and both can be visually represented in Fig. 3.13.

To create lower impedance levels in the HaptX G1, the PWM control of the 8 lbs finger lock was used as described in subsection 2.2. The HaptX gloves were not designed for this

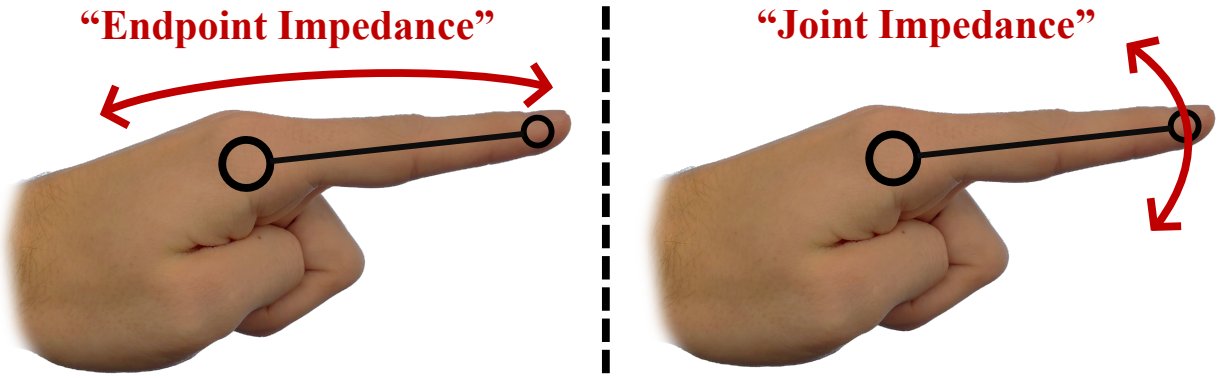

Figure 3.13: Representation of endpoint versus joint impedance on the MCP in this experiment. While both impedance types may be inflicted at the endpoint of the user's finger, where the internal reactions are felts is what defines the impedance name. In both cases shown, the index finger is fully rigid, so the MCP joint is the only one experiencing a difference in impedance.

use case, and many of the sounds and feelings created by running the PWM control can be used to easily tell that the HaptX is active. Since the experiment's sole purpose is to test the subjects ability to differentiate *impedance types* not *which robot is being used*, multiple effects had to be eliminated or at least mitigated to gain useful information from the experiment.

The HaptX glove finger locks use a solenoid to open/close the valve responsible for inhibiting finger movement. The actuation of these solenoids can be felt along the back of the wearer's hand, especially when repeatedly actuating, such as in PWM control. The actuation of those solenoids also creates a loud clicking sound, which can very easily be used to audibly distinguish which device is enabled. To minimize the audio effects, subjects donned over-ear headphones playing white noise during the entire experiment. To minimize the back-of-hand haptic effects, the middle finger of the HaptX glove was running PWM during the entire experiment. Subjects were then asked to move both their index and middle finger together during the entire study, while only using the difficulty of moving their index finger to make their decision. This creates the haptic 'clicking' effect of the PWM controller on the HaptX during the entire experiment, instead of just when the HaptX is controlling the subject's index finger.

Regarding controls, while SER operates at 480 Hz, the HaptX's PWM operates at a 30 Hz period, meaning subjects could just use the perceived 'smoothness' of the impedance felt in their index finger as the factor used to discriminate devices. Initial pilot testing of these effects with both devices running at full capacity revealed that not a single tester failed to distinguish between impedance types, so modifications to SER to decrease its smoothness and hide external physical effects of the HaptX were made. To compensate for these operating frequency differences, the SER control gains were increased and the control was enabled/disabled at 30 Hz, the PWM period of the HaptX. This eliminates subject's ability to differentiate continuous and discrete control as a factor in the experiment.

While SER's bandwidth easily covers maximum human movement frequency [45], the HaptX PWM control cannot. As the index finger is moved at higher frequencies, the magnitude of both the haptic and audible effects created by the HaptX dramatically increase, ruining immersion and making it near impossible to fail to distinguish from SER. To avoid the participant's from approaching the limit of HaptX control, they were provided a 60 BPM metronome and were advised to match their finger movements with the metronome.

With all control modifications and sensory deprivations imposed on the user, the binary discretion experiment can reveal strictly if users can differentiate between the different impedance types created by the different devices.

3.4 Experiment to Determine Human Impedance Differentiation Capabilities

To understand human capacity to differentiate between joint and endpoint effects/impedances, an experiment where touch alone is used to differentiate between devices over multiple trials was conducted. This section describes the experiment, including protocol, results, and how those results impact the existing knowledge.

3.4.1 Experimental Protocol

In accordance with Auburn University IRB Protocol #00000269 this study involved the participation of ten healthy subjects between the ages of twenty and thirty with no known physical or mental impairments. The use of healthy participants was necessary to provide an appropriate measurement of impedance detection capacity of the general population.

Each subject was seated in a chair facing the SER and next to the HaptX G1 air pack. Users then initially placed their hand on SER's hand rest, fully extended their index finger, and the hand rest was adjusted front to back by the tester to fit SER to the subject. The subject then donned a mesh glove liner before donning a left hand G1 glove, which was then secured by the tester using the built-in cabling and straps on the G1. Users then set their hands back on the hand rest and clipped their finger into SER, similar to what is shown in Fig. 3.3.

Each experiment began with the subject participating in serial exploration [46] of each environment in a known order:

1. (20 sec) Stiff environment created by SER
2. (10 sec) Break with no finger movement
3. (20 sec) Stiff environment created by HaptX
4. (10 sec) Break with no finger movement

Providing them with insight on the feel of each device. Subjects were encouraged to move their fingers along with the 60 BPM metronome playing in their headphones and were also advised to move both their middle and index finger simultaneously to further isolate the key distinguishing factors to which device was creating the stiff environment for their index finger.

A virtual stoplight was shown in front of subjects on a computer monitor, displaying a different colored light for each 10 second segment of the 30 seconds trial, where each trial

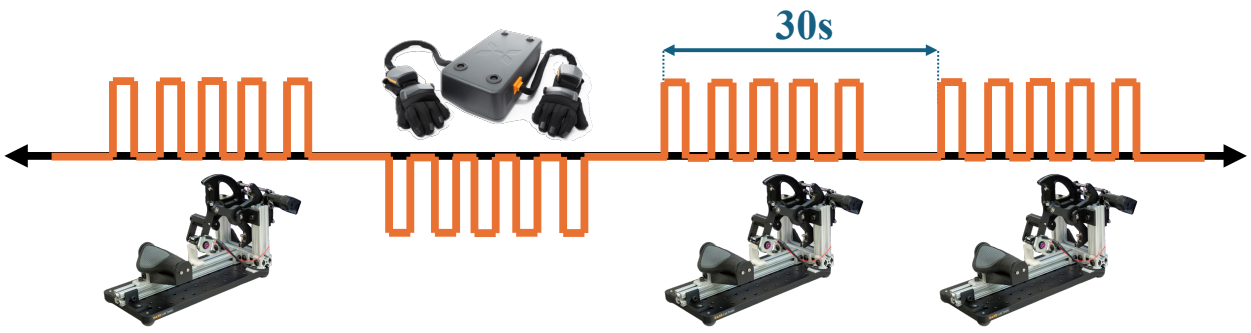

Figure 3.14: An example of a possible control exchange over the course of four trials during the binary discretion experiment. A device (and thus, an impedance) was randomly chosen to be enabled for 20 seconds, with a 10 second break between active periods.

can be seen highlighted in Fig. 3.14. The lights and what they mean were disclosed to the subjects before the experiment began and are as follows:

1. ('Green Light' - 10 s) Subjects participated in serial exploration to determine which impedance type was rendered

2. ('Yellow Light' - 10 s) Subjects refrained from movement and vocally declared the impedance type they believed was rendered

3. ('Red Light' - 10 s) Subjects were asked to not move at all and wait for the next section

For each trial, the impedance type and participant's respective guess were recorded.

3.4.2 Results

All ten subjects participated in the single-experiment, ten trial binary discretion experiment and filled out a survey about the experiment located in the appendix. The primary data collected results in Fig. 3.15, where subject's cumulative discretion accuracy over the ten trials is recorded along with the number of participants per final accuracy. The experiment results display that participants *could* discern a difference between joint and endpoint impedance, whether immediately or after multiple trials.

The cumulative accuracy results shown in Fig. 3.15 reveal both a high-accuracy, seven-participant 'primary' group and a low-accuracy, three-participant 'secondary' group. The

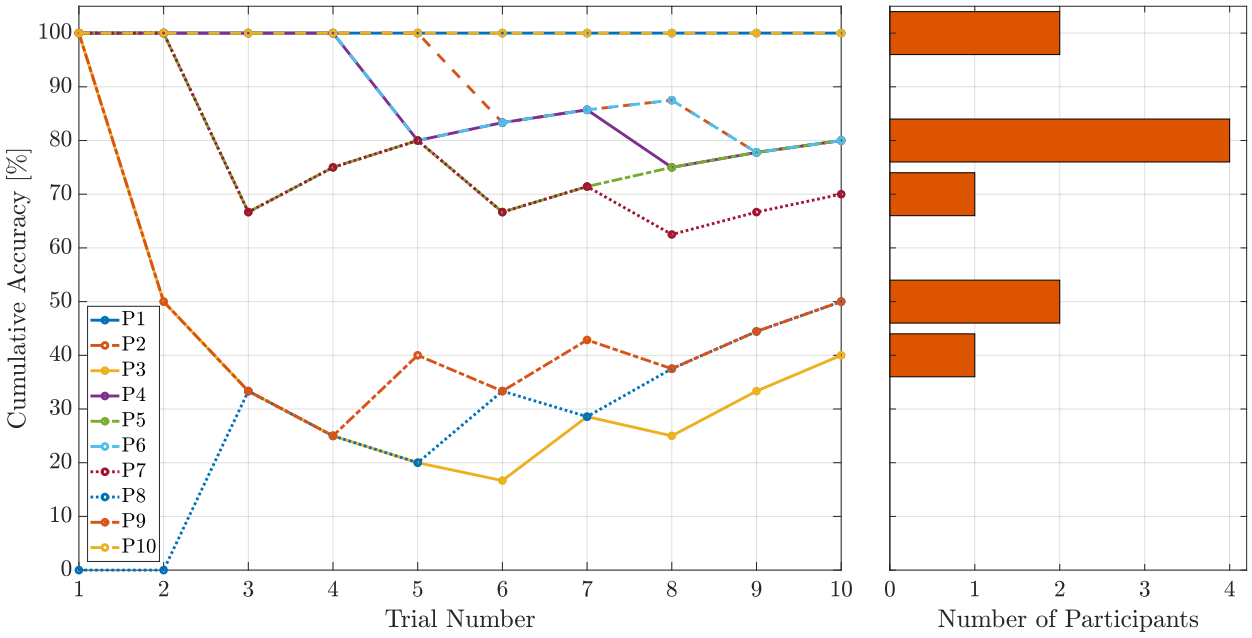

Figure 3.15: Progressive accuracy during testing trials, and final accuracy over ten trials - per participant. Across the cumulative accuracy, the subjects can be visually broken in to two groups: higher (70% and above) and lower (50% and below) accuracy. The two groups can be seen in the number of participants per final accuracy metric on the right, where the most common accuracy was 80% with few outliers on either side.

primary group finished with an average accuracy of 84.3%, and the secondary group finished with an average accuracy of 46.7%. All non-perfect participants were increasing their accuracy at an average rate of 3.47% per trial from the 9th to 10th trial.

Cumulative accuracy was chosen as the primary metric as it highlights how the subjects approach a true discretion accuracy value as the experiment progressed. Similar to other haptic discrimination/learning experiments like the co-activation experiment of Dinse et al. [47], the participants increased their discrimination ability even with no direct feedback on which device was active/inactive during the experiment. This implies that an extended experiment with more trials could yield much higher average accuracy, regardless of initial participant accuracy (first 1-5 trials). Alternatively, a shortened or eliminated serial exploration period could cloud discretion accuracy.

Out of the ten tested participants, two of the three participants who scored 50% or less noted mentally 'swapping' what the HaptX and SER felt like early in the experiment,

and then over-corrected halfway through. Their cumulative accuracy confirms this, as they were each increasing in accuracy at a faster rate than the primary group from trial nine to trial ten. This means that although this secondary group had a lower average accuracy of 46.7%, this is not the result of not being able to differentiate between the SER and HaptX, but instead because of the nature of the experiment: being forced to rely on only a brief introduction to each device and initially only having that information to make one's decision. The implication of this for future SER experiments is that the manipulation of exposure time could very likely increase or decrease discretion accuracy.

3.4.3 Discussion

From this experiment it can be concluded that most people can tell the difference between joint and endpoint impedance as rendered by SER and the G1. Not only do the accuracy metrics in Fig. 3.15 point to high discretion accuracy, but they also highlight an improvement over time by participants. As there are no known gloves which outperform the G1, this means that at the time of publication, there is a need for a multi-finger *joint* impedance device (such as a five-fingered version of SER) for an immersive RA simulation. Before the creation of such a device, there are various experiments that should be conducted to further understand human ability to differentiate impedance and to depict device impedance quality and magnitude.

Regarding overall accuracy, subjects 3 and 8 both reported a realization of their internal bias mid-experiment, meaning that 90% of subjects (subject 9 as the only unexplainable low accuracy) declared having a confident idea of which impedance type was influencing their index finger by the conclusion of the experiment. Given the progressive accuracy increase from the 9th to 10th trial it can be hypothesized that, had more trials been conducted, accuracy would continue to grow for all participants, likely reaching an equilibrium point between 80% and 90% accuracy.

3.5 Future Work and the Next Version of SER

Even after concluding this study, there is still a lot of room for improvement and extended experiments in the realm of impedance differentiation. This section breaks down what those experiments could look like, and the future of the SER project.

3.5.1 Future Experiments With the SER and HaptX

To validate this hypothesis, a direct extension of this experiment should be conducted. This experiment would involve participants repeatedly going through trials until reaching a minimum accuracy change threshold (with a defined minimum percent change) would reveal a 'final' accuracy value, on average. Data from such an experiment could be used both to validate the results of this study, and to determine an average amount of serial exploration needed for a participant to become aware of the different impedance types. Fig. 3.16 visualizes what this extended experiment could look like, both in exploration and testing trials.

Figure 3.16: How the SER experiment could be extended, both in serial exploration and number of testing trials. The extension of the serial exploration segment could increase discretion accuracy, and extending testing trials may reveal the true average discretion accuracy.

Also, it may be valuable to understand the relationship between explored region of device control and overall participant accuracy. In the binary discretion experiment of this paper, the controllable region of devices that the subjects explored during their 20-second exploration period was not recorded, but a version of the experiment where exploration area was recorded could reveal more insights into what makes a human accurate in their perception. A single pilot test with these new conditions, resulted in an initial exploration of

51% of SER's range-of-motion and an accuracy of 70% by the end of the ten trials. Further tests with quantified exploration must be conducted to plot and discover trends between exploration and discrimination accuracy. The results from such an experiment would likely provide an insight in to what participants use (time, exploration region, etc.) to learn the difference between joint and endpoint, or if stripping them from any of this exposure could hide any differences for an RA simulation.

If these proposed experiments instead *contradict* the results of this study, further investigation would be required to see if a device like the HaptX could be used for an RA simulation. Because the HaptX is not designed to create lower or varying levels of impedance, it generates significant haptic and audible artifacts that impact saliency. A few key mechanical improvements could be made to reduce these artifacts. First, the HaptX finger locks must be able to operate at a higher PWM period than 30 Hz. The value of this frequency can be experimentally determined through a future JND experiment using SER and progressively smaller PWM periods. Also, the HaptX G1 can only run the 30 Hz PWM control on two fingers without sacrificing power, but the air pack must be able to deliver and actuate enough air to create impedance in all five fingers per glove for an effective RA simulation.

3.5.2 What a Multi-Fingered Version of SER Could Look Like

The results of this experiment point towards the eventual need of a new version of SER, one that is capable of creating joint impedance for each finger in an ungrounded environment. Due in part to the inverse relationship between size and power, this could prove to be extremely difficult. Not only that, but generating impedance not just for the MCP joint but for every joint of the fingers would significantly increase the complexity of the system.

Because of these reasons, there is significant drive to see if visuohaptic effects could be enough to blend the stiffness generated by some multi-fingered SER. By mismatching the avatar with the real user, visuohaptic effects could create the illusion that the users hand

may be stiff along all joints while the MCP is the only real joint experiencing stiffness. This is furthered by the fact that the primary joints that RA inhibits are the MCP and distal interphalangeal (DIP) joints.

Therefore, it's likely that a multi-fingered version of SER would include multiple smaller, lower-power, lower-torque, rotating four bars that are mounted on the back of the hand in combination with a virtual reality program specifically designed to not match the user's body. A device similar to the existing Maestro glove [48] [49] to inhibit the wearers MCP and DIP joints provide an example of a device designed for such emulation.

Chapter 4

CASET - Curling Artificial Soft ExoskeleTon

Lifting heavy objects imposes complex stresses on the musculoskeletal system, leading to grip fatigue and eventual failure over extended carry distances. Although existing commercial off-the-shelf products can partially alleviate this stress by offloading it to the wrists, they lack the ability to retract and remain unobtrusive — a critical requirement towards adoption and long duration use. CASET, a novel solution that integrates fundamental electromechanical principles to offload loads of 25lbs per hand. CASET was evaluated in an experiment where users held 25lbs dumbbells to failure both with and without the device where they displayed significant improvements to both hold duration and grip fatigue reduction.

4.1 Background - The Need for an Assistive Litter-Carry Device

There are many reasons to develop an assistive device in litter carry units, and this section distills those reasons and why existing solutions may fail to meet the desired performance.

4.1.1 Relevant Literature

In search-and-rescue operations, litter carriage transport is an essential part of relocating the injured to a safer area [50]. As this task is usually done on foot, when covering long distances litter carriers may experience significant stress on their upper extremity joints and hands, and long-term musculoskeletal injuries may develop over time as a result of extended litter carry which could impact the performance of those groups [51].

In a recent study by Madison et al., 15 military-active participants participated in an experiment to evaluate litter carry time over multiple trials to assess fatigue and test off-the-shelf solutions. The results of this study confirm the hypothesis that these litter carry groups experience fatigue over long distances and multiple carries. Therefore, in the same study, off-the-shelf alternatives to relieve the fingertip stress were tested revealing up to 27% grip strength fatigue reduction.

While this study points towards using assistive devices in litter carry groups, many of these devices are always-enabled and remain obtrusive when the carrier may need to convert to dexterous tasks immediately following carry. Therefore, a new solution is desired with the caveat that it must still drastically improve grip fatigue and carry time, similar to the tested alternatives.

4.1.2 What Current Solutions Lack

The current state of the art in increasing grip strength is either exoskeletons (e.g., SPAR [2], Carbonhand [52], Bioservo [53], etc.) or harnesses [54]. Further description of these alternative devices can be seen referenced in the background of this manuscript in subsection 2.1.2.

In an environment where quick donning/doffing of the device and its load carrying, an over-the-shoulder harness lacks the ability to quickly engage/disengage with its load, leaving the user potentially tethered to the load once they've transitioned to their next task. Wrist-mounted hooks have a similar issue: there is no efficient way to get the user out of the load *and* get the hooks out of the way of any dexterous movements that the hands must be available for.

In many fields where robotics and exoskeleton technology are being applied, many are searching for an electromechanical solution to jump the gap between the current SoTA and the actual desired device [4]. Hand-based systems like the SPAR-Glove [2], originally designed for stroke rehabilitation, could be modified to create a new optimal device or

improve existing solutions to match the new requirement of quick don/doff. Such a device could reduce grip fatigue, but would require validation through a comparison with and without the device, understanding of system usability by test subjects, and investigation of EMG signals to understand muscle activation during hold [55].

4.1.3 Contributions

This chapter covers the design and experimental validation of a supernumerary robotic hand that meets proposed design criteria: CASET. In section 3, the design of CASET and its primary inspirations will be described along with figures of both 3D models and real-world versions of the device. Section 4 covers the experiment used to validate both CASET's proposed reduction to grip fatigue and improved carry time of a pair of 25lbs dumbbells, and the results of said experiment. Lastly, in section 5 the results of the experiment and why they show enough improvement over base human performance enough to validate a future iteration of CASET will be outlined.

4.2 Design and Working Principle of CASET

This section breaks down the development of CASET and its various working principles and design inspirations.

4.2.1 Design Requirements

To exceed performance of existing lift solutions, CASET must meet a series of design requirements. Meeting these requirements through pilot testing and the study completed in section 4.3 will suffice in validating CASET and the potential for future work in litter carry assistance exoskeletons. Table 4.1 displays the desired performance metrics from the device.

Table 4.1: Description of design requirements for the CASET device.

Performance Metric	Value
Carry capacity (per gripper)	$>$ 25lbs
Carry Time Increase	$>$ 100%
Grip Fatigue Reduction	$>$ 25%
Time to activate	$<$ 10s
Power consumption while holding	$<$ 10Wh

4.2.2 CASET Version History

CASET is the product of half a year of innovation, prototyping, machining, printing, and more. Initial testing of the core working principles naturally turned into final concept development, integration of these principles, and pilot testing. This subsection breaks down the history of development for CASET through various prototypes and CAD models.

The first step in CASET prototyping was to understand the trapezoidal links of the SPAR glove from Rose, so a mock up version was printed and tested seen in Fig. 4.1. Multiple versions of these 'fingers' were printed a tested to understand how different geometries impacted performance. It was later determined that the actual CASET grippers needed to be significantly taller to create a much larger moment arm between each link to hold the desired weight.

To compliment the fingers being prototyped, the first linear actuator prototypes to drive them were developed. The actuator prototype in Fig. 4.2 was made from a printed PLA box, and instead of using linear slides relied on a diamond shaped carriage that rode between embossed rails on the top and bottom of the box. This worked, but under high loads (inflicted by holding on to the cable as the motor was powered) created too much friction which inhibited actuation.

The entire linear actuator and electronics system can be seen in Fig. 4.3, where rubber lines were used to route the steel cable, and the core electronic components were tested on a breadboard.

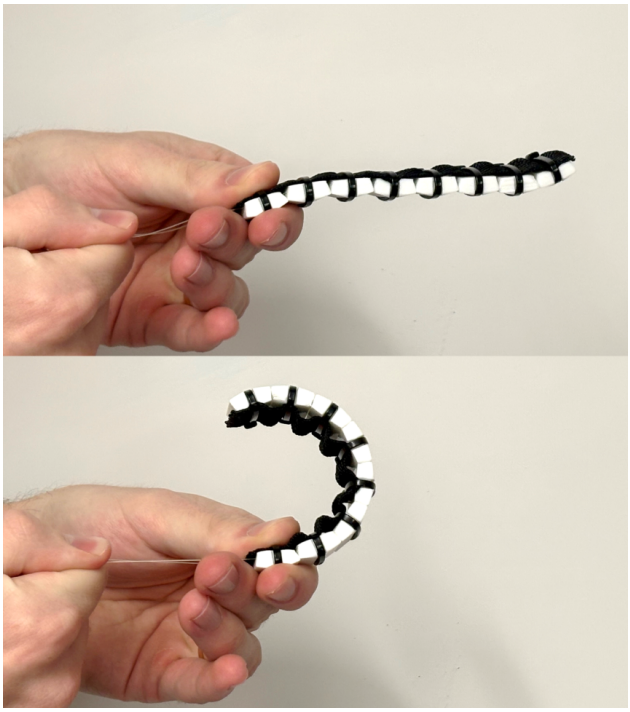

Figure 4.1: The first of many trapezoidal link prototypes to test the core working principle of CASET. By pulling the routed fishing line, the 'finger' curls up, and can be held in that state under constant tension.

The system can be seend worn by a user in Fig. 4.4. This prototype could move the linear actuator in and out, retracting and extending the cable as designed. However, the previously mentioned embossed rails and unrealistic size of the electronics which were developed on a breadboard would require changes in the next version of CASET.

To reduce friction, small metallic linear slides with ball bearing sliders were used, as seen in Fig. 4.5. There was also a thrust breaking located in the end plate of the actuator to hold the lead screw as the device was loaded. This version of the actuator was the first to incorporate Jagwire for steel cable routing to the grippers.

Seen in Fig. 4.6 is the first fully-working gripper prototype that was not just an individual 'finger'. Driven by the actuator in Fig. 4.5, this gripper could hold 10-15lbs, but the thin printed walls of the actuator would snap and break at the screws when loaded any higher. The slits in this version of the gripper were intended for routing canvas material through for

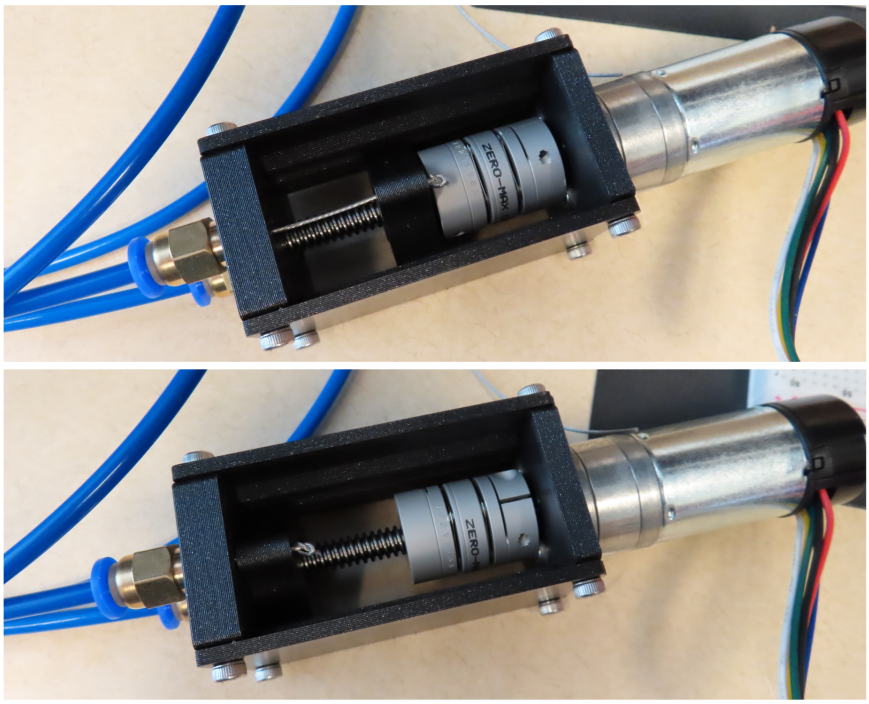

Figure 4.2: The first version of the linear actuator. This version was a simple prototype to test the actuator style, and used rubber lines as Bowden cables to guide the steel cable.

a cleaner interface with the litter, but these were scrapped for the foam padding seen in the final CASET version later.

Enough information had been learned after the development of all previous CASET prototypes to begin working on the final CASET version.

The electronics of this CASET version were identical in content to early prototypes, but they were organized in a much more compact manner to fix in the printed electronics box shown in Fig/ 4.7. This box contained the motor controller, voltage limiter, current sensor, on/off switch, and Raspberry Pi Pico.

The final version of the CASET linear actuator, seen in Fig. 4.8, was designed to be manufactured from 6061 aluminum, as the wall that bears the load of the lead screw in the actuator is the first failure point of the device under excessive loading. However, the box is also fully 3D-printable with the caveat that it can hold lower weights. Physical prototypes of CASET manufactured from aluminum could comfortably hold 55lbs, and printed versions 30lbs.

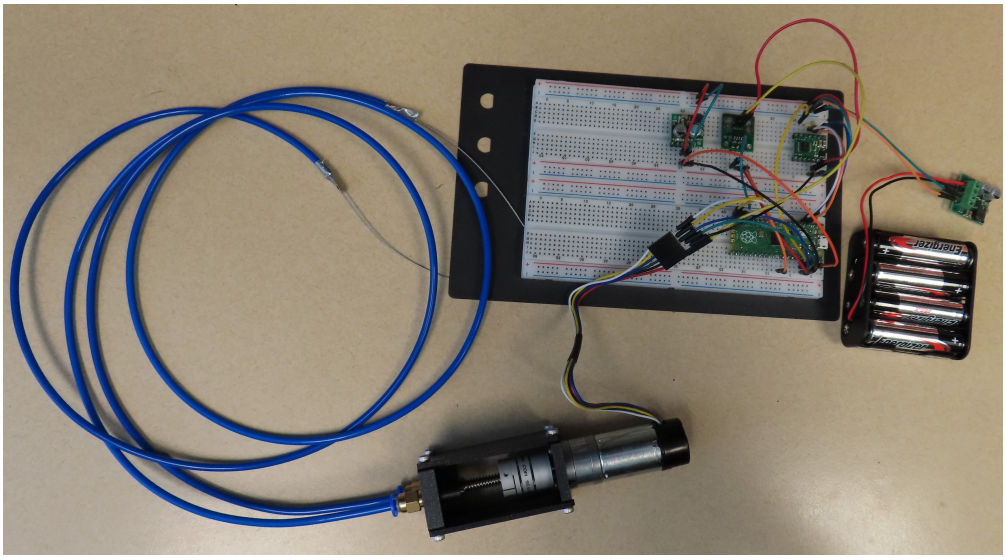

Figure 4.3: Overview of the first working CASET prototype. This version did not bear any load, but the actuator was controllable using the Pi Pico.

Combining the actuator, grippers, and electronics box results in the final version of CASET seen in Fig. 4.9. The system, with the aluminum actuator box, was capable of holding 55lbs per gripper, and could be stowed in the arm mounted gaiters as shown in the figure.

This version of CASET and its components are further broken down in the following section.

4.2.3 Working Principles and Inspirations

To redirect load from the fingertips to more fatigue-resistant parts of the body while also maintaining the ability to extend and retract on-command, a novel robotic device was created: CASET. CASET Works like a weightlifting hook: by offloading the carry load from the fingertips to the wrists grip fatigue is reduced and the user is capable of holding the load for an extended period of time.

What CASET can do that weightlifting hooks are incapable of is extending and retracting on-demand via a powered linear actuator and geometry manipulation. The hooks at each wrist of CASET 'curl' when enabled, forming a rigid C-shape and thus behaving like a

Figure 4.4: Overview of the second working CASET prototype. This version could hold 10-20lbs dumbbells, but when weight was increased any more the 3D printed parts would fail under loading.

weightlifting hook, but when the user does not need CASET's assistance, they may disable the device and the hooks 'uncurl' and become loose, allowing the user to reroute the hooks to avoid imposition.

The curling motion of CASET's hooks is primarily inspired by the SPAR-Glove design which uses trapezoidal 3D printed linkages with a steel cable running between them to turn the tension from the cable into curling force. With sufficient cable tension, and under low enough load, the tensioned hook acts as a rigid body, supporting and offloading the force from the fingers to the wrist [56]. CASET works via a custom, back-mounted, linear actuator that tensions a steel cable to curl the hooks located at the wearer's wrists. When enabled, these curled hooks can hold the carry load, offsetting the stress of holding said load from the wearer's fingers to their wrists and can be seen in Fig. 4.9.

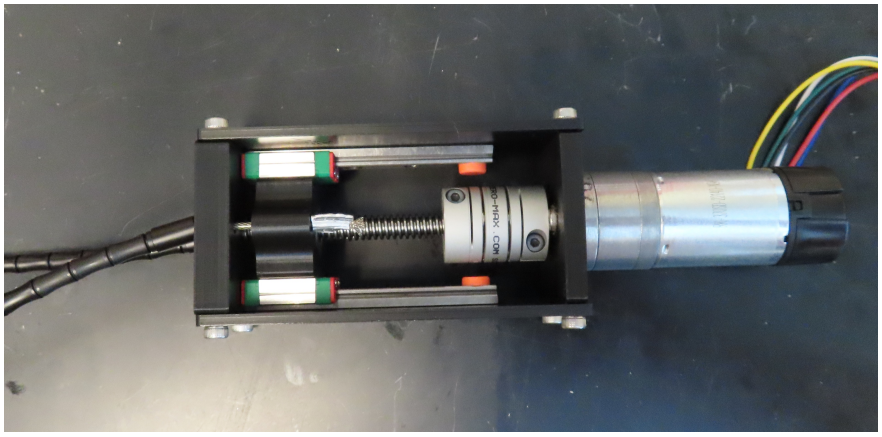

Figure 4.5: The updated actuator with linear slides for increased strength and reduced friction. This version was also the first one that implemented the Jagwire Bowden cables.

4.2.4 Design Breakdown

CASET can be broken down in to three primary components: the back mounted linear actuator, the Bowden cables linking the actuator to each hook, and the two hooks each mounted to the wearer via a hook and loop strap.

The first step of CASET actuation is the powering and control of a back mounted linear actuator to tension the cables that curl the hooks for stress offloading, similar to that of [57]. Off the shelf linear actuators are expensive, bulky, and loud, so a custom, smaller form-factor actuator was desired for this application.

The version of the CASET linear actuator used in this study is housed in a 3D-printed, polylactic acid (PLA), box printed at 50% rectilinear infill with 5 perimeters at a 0.1 mm layer height on a Prusa Mk4 [42] printer with input shaping. This box was designed to be manufactured out of 6061 aluminum to improve its ability to withstand the high loads imparted by the cable tension, especially along the axis of rotation of the lead screw. However, the manufacturing and materials for such a box are much higher than that of printing the box in-house, so this version of the actuator maintained the 3D-printed form of the prototypes before it.

The actuator is powered by a Pololu 12V Brushed DC motor with a 75:1 metal gearbox and measures rotations via a 48 count-per-rotation encoder, thus providing a 0.1 degree

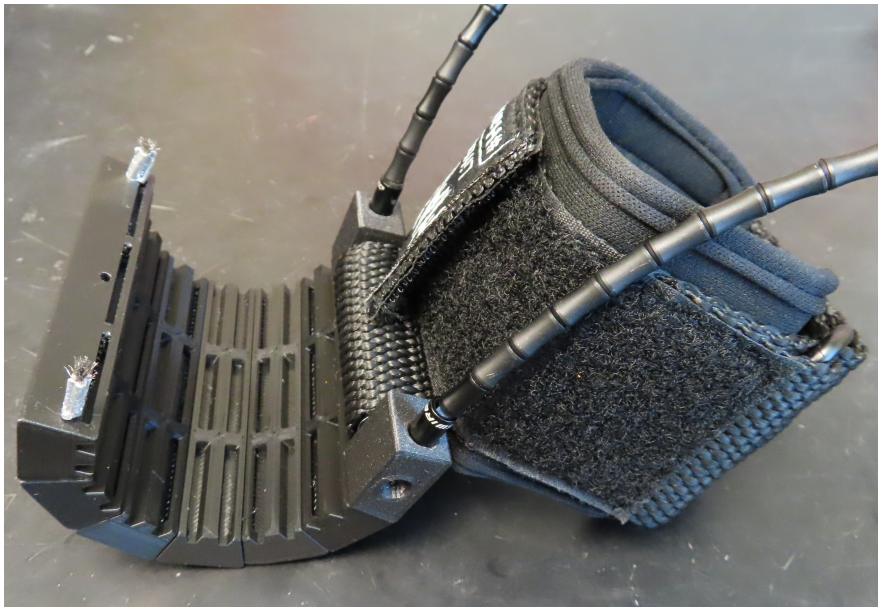

Figure 4.6: The first working CASET gripper. This version was large to overcompensate for the force requirements and included slits for straps to run through.

resolution. The motor connects to a lead screw using a shaft collar which is supported at the other end of the box with a thrust bearing. On the lead screw, a press-fit nut in a printed PLA block holds the steel cable that is tensioned by the actuator. The linear actuator retracts a single 1/16" diameter steel cable that runs throughout the entire system. The cable begins and ends at the sliding block inside the actuator, and is routed through a total of four Bowden-cable [29] enclosures created using Jagwire [31] and linking the movements of each gripper to each other using shared tension. As the block is retracted "up" the lead screw, the tension in the cable grows, and the curling motion in each hook commences at a rate proportional to the block's change in displacement. The box containing the linear actuator is designed to be manufactured from 6061 aluminum, but the prototype evaluated in this study uses 3D-printed PLA.

The tension in the steel cables is what is used to create the curling motion of the CASET device. Each gripper is composed of a hook-and-loop wrist strap which has a series of 3D-printed PLA blocks (printed at the same specifications as the linear actuator box). As seen in Fig. 4.11, the grippers curl as tension increases and as the cable 'shortens' in length relative

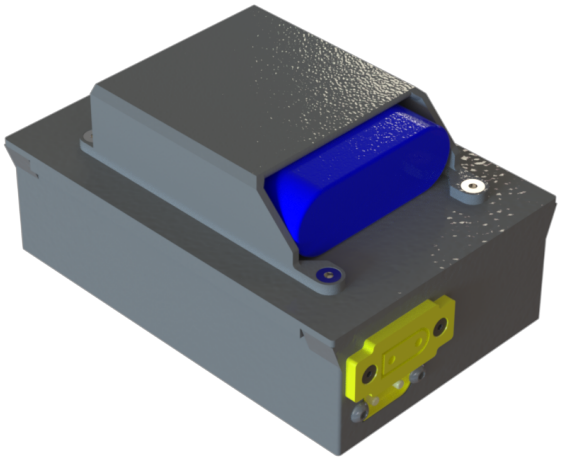

Figure 4.7: The final version of the CASET electronics box. This box contains a 12V battery holder and enough room for all the system electronics to fit comfortably. It mounts to a standard MOLLE vest using straps and buckles.

to the gripper. This SPAR-Glove-inspired motion is a result of individual moment arms created at the intersection of the edges of each trapezoidal link by the tension of the cable. Each individual trapezoidal segment of the hook has a steel cable running through it which is anchored at the last link. As the cable is pulled tighter via the system's linear actuator, the segments come closer together to create a "curling" motion. When fully tensioned, the hook acts similar to a rigid weightlifting assistance hook, offsetting load from the fingers to the wrists. The grippers act rigid under loads of up to 25lbs, based on design requirement.

The CASET system runs on a Raspberry Pi Pico [58], and the electronics system can be seen in Fig. 4.12. The device internals include the previously described motor controller, a voltage regulator, power switch, Pi Pico for controls, and a 12V battery (not pictured).

The CASET system runs using simple on/off control. The device was designed with the intent that the friction of the lead screw in the linear actuator would prevent the actuator from backing out and prematurely releasing the CASET grippers. When the user presses the 'enable' button located on the wrist, the DC motor operates at full power until it reaches a current draw of 4.9A (98% motor stall torque) and the actuator is considered 'fully actuated'. This is done to eliminate any variation in cable lengths when CASET is enabled, since the actuator pulls the cable up to the same tension regardless.

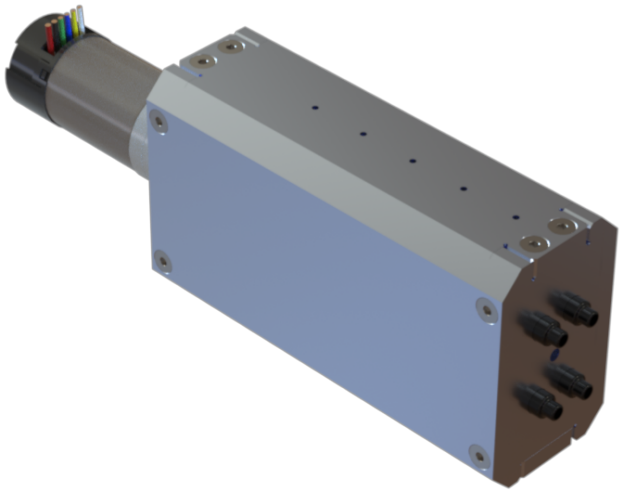

Figure 4.8: The final version of the CASET linear actuator. The actuator was designed to be manufactured out of aluminum, but is also fully printable out of PLA, with a significantly lower failure point under loading.

To evaluate the size, weight, and power (SWaP) of CASET, measurements were taken along with a simple pilot test for current draw. Seen in Fig. 4.13, CASET can fit within a 200x250x300mm box and weights 1.81 Kg, with most of that weight proximally located on the back where the linear actuator and electronics are mounted.

For power consumption, a simple experiment where CASET was curled/uncurled three times and current draw was measured during each cycle was conducted. The results of this experiment seen in Fig. 4.14, where the 8-second-each actuation steps combine for a total power draw of only a fraction of the 1200 mAh battery used. The system can hypothetically run a total of 540 cycles before needing a full charge, but effects of battery drain on motor strength and actuator pull still could be measured.

4.3 Experiment to Validate Performance of CASET

To validate the design requirements of CASET, a human-subject experiment to compare innate human performance with the use of CASET was conducted. The experimental procedure and what data was collected is outlined in subsection 4.1, and the results of the experiment are displayed in subsection 4.2. A discussion and breakdown of future studies and

Figure 4.9: The Curling Artificial Soft ExoskeleTon (CASET). CASET is a lift-assistance device that offloads carry weight from the fingers to the wrist to increase carry time and reduce fatigue. Front (left) and rear (right) views shown in the enabled and disabled states respectively.

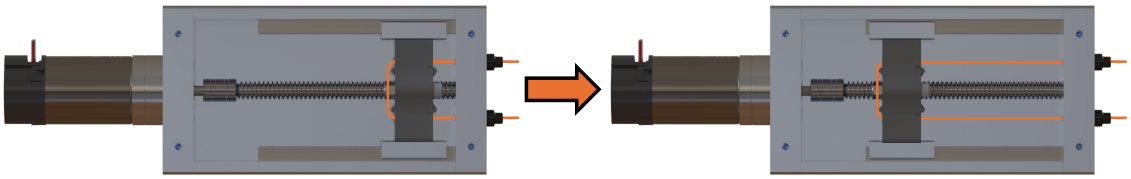

Figure 4.10: The back-mounted linear actuator. Using a lead screw and nut, the brushed DC motor driven actuator retracts a 3D printed block which holds the cable that runs through the entire CASET system.

design improvements are described in subsection 4.3, where the next steps and "CASET 2.0" are shown. Overall, the experimental results point to significant carry time improvement and grip fatigue reduction, but response from participants underline a need for improvements to the ergonomics and operation of CASET.

Figure 4.11: The CASET grippers, in CAD and reality. The SPAR-inspired working principle can be seen in action through the curling motion when tension is applied.

4.3.1 Study Procedure

The ten-participant study used to evaluate CASET against unassisted subjects consisted of a carry time test, grip fatigue evaluation, and a system usability scale to get direct feedback on the operation and potential improvements for CASET [59].

Ten participants with no significant physical or mental injuries or inhibitions who were capable of holding up to 25lbs per hand while sitting down were evaluated using multiple sensors and systems. Initially, the Deslsys EMG sensors [60] used to evaluate the flexor digitorum superficialis (FDS) and extensor carpi radialis (ECR) muscles for each the participant's left and right arms during the study were normalized. This was done in a standard maximum voluntary contraction (MVC) initialization process where the participant's hand was anchored to a 50in tall wooden platform by an assistant and the participant tried to lift their hand from the box as hard as they could in either pronation or supination to activate either the FDS or ECR muscle group respectively. Each MVC was taken three times per

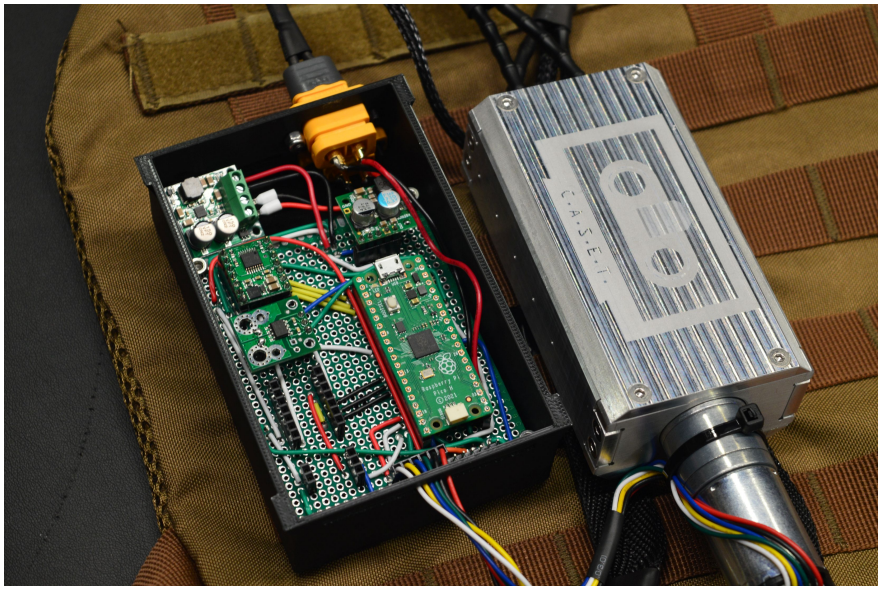

Figure 4.12: The CASET electronics and aluminum CASET version shown on a tactical vest. The electronics were soldered to a solder-less breadboard to connect each component.

muscle group, and the largest and highest magnitude section of contraction was automatically selected as the MVC for each muscle, of which EMG signals during the experiment would be compared to.

After the MVC of each muscle group was taken, participants were seated in a chair with two 25lbs dumbbells placed on foam pads to their left and right as seen in Fig. 4.15. Participant's grip strength for each hand was then evaluated using a Jamar grip dynamometer [61] to get a before-experiment measurement as a baseline to see how much their grip was reduced after holding the weights.

Participants were then provided the weights by those running the experiment and immediately as the weights were handed off to them a timer began. Subjects were instructed to hold the weights as long as physically possible and to just drop them on the foam pads when they were done. When the subjects dropped the weights the timer was stopped and new grip dynamometer measurements were immediately taken within seconds of the weights being dropped. During the entire hold period, EMG signals were being recorded from the FDS and ECR muscles.

Figure 4.13: Size and weight measurements for CASET. Size measurements took into particular consideration CASET's transportability, so the smallest box the entire device could reasonably fit into was measured.

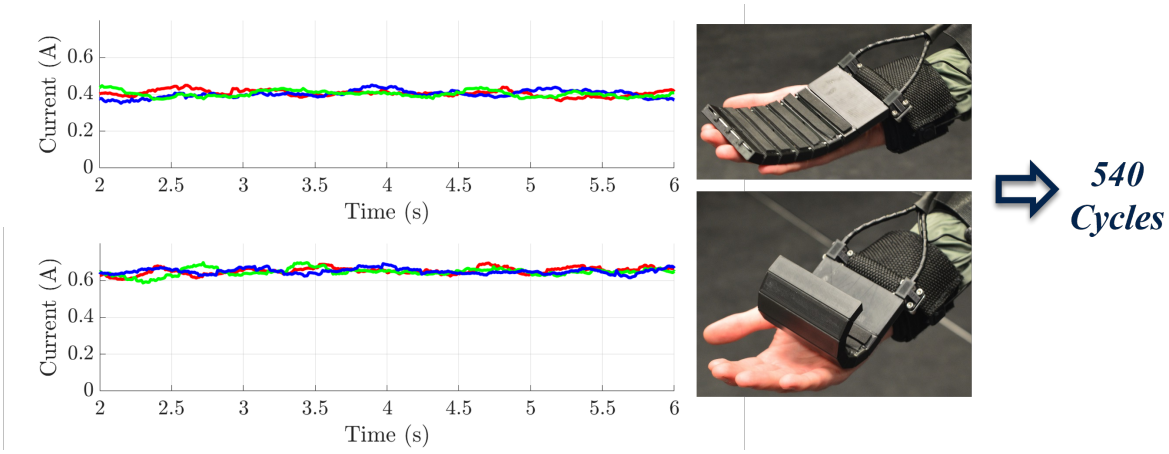

Figure 4.14: CASET Current draw during the curl and uncurl steps. The total cycles this power draw results in is shown as 540 cycles.

After a five minute rest period, the exact same experiment was then repeated with the CASET device. Participants donned CASET with the help of testers via the hook and loop wrist straps attached to the grippers, while the actuator sat in a chair behind the participant. CASET was enabled during the entire don/doff process and during data collection.

Five of the ten test subjects were evaluated without CASET first and with CASET second, and the other five vice versa. This helped us find any issues with the experiment, such as the break period between tests not being long enough, and potentially even evaluate the two groups independently to mitigate any impact of these issues.

Figure 4.15: User interaction before and after holding weights with CASET. After the participant begins by lifting the weights slightly, testers pull the weight stands away and replace them with foam pads for the participant to release the weights upon.

After conducting both carry time experiments and collecting all relevant data, participants were asked to fill out a standard system usability scale on the CASET device which would be used to critically evaluate CASET from the perspective of an actual user. The culmination of all experimental procedures and data collection provided us with the following information: grip strength before and after both carry time tests, time-to-failure for both tests, EMG signals of the FDS and ECR muscles for both tests, and system usability scale results. All of the collected data is displayed in the following subsection 4.2.

4.3.2 Results

This study was conducted on a total of 10 participants with an average weight of 74.3±14.0 kg and average height of 1.72±0.1 m. Since participants were only given five minutes between holding trials, they were split in to two groups of five to avoid lingering fatigue from after the five minute break from significantly impacting data collection. The first group held to failure without CASET first, and the second group with CASET first. Fig

4.16 shows the hold times for each participant both assisted (with CASET) and unassisted (without CASET).

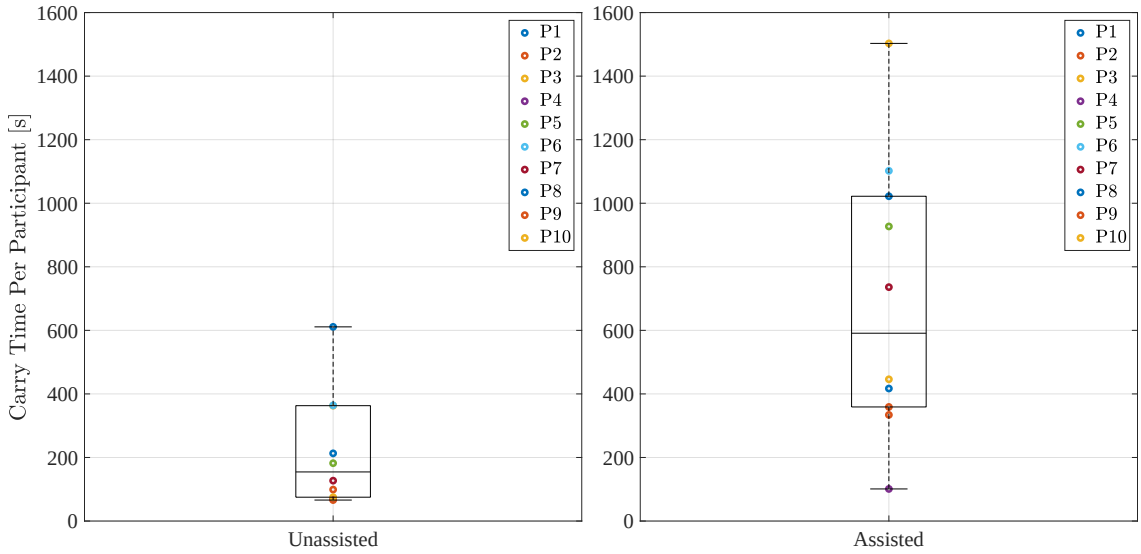

Figure 4.16: All carry times both assisted and unassisted for all participants. Even numbered participants used CASET first, and odd numbered used CASET second.

These carry times were evaluated on a per-participant basis to see improvements as a percentage increase. Fig. 4.17 displays carry time percent increases when using the CASET device compared to when holding the weights empty-handed.

The average carry time increase was 221% for the CASET second group and 338% for the CASET first group, a significant increase. As expected, the group that used CASET first held the weights for longer time than the group that used CASET second. This is because when holding the weights first and using CASET second, subjects experience lingering fatigue that impacts their comfort and ability to last when holding with CASET. Since in a real-world setting, users would not have previously experienced muscle fatigue, there should be a performance increase somewhere in between each group.

However, carry time increase is not the only objective of CASET. The device must also be capable of reducing grip fatigue thus allowing for easier transition to dexterous tasks and lowering the odds of long-term injury. Fig. 4.18 below shows the percentage reduction in

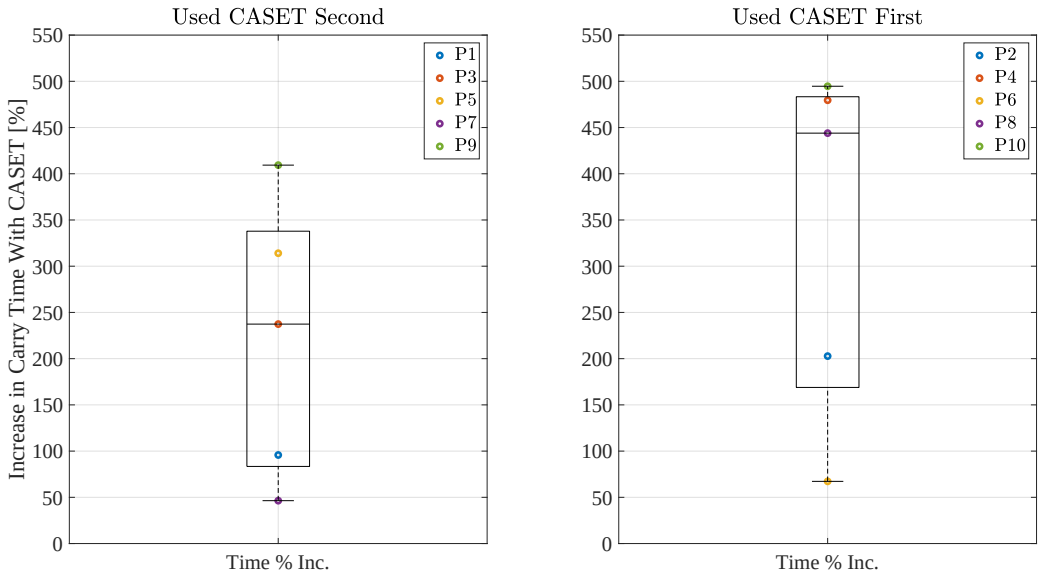

Figure 4.17: Carry time percent increase when using CASET to failure. 100% of participants experienced increase in carry time when using CASET, with many experiencing a triple or quadruple increase.

grip fatigue from their with CASET to without CASET trials, with the 5-subject groups plotted separately:

Grip fatigue reduction is measured as the loss of grip strength from holding the weights to failure without CASET compared to the grip strength lost from holding with CASET. As anticipated, the group that used CASET second experienced a larger reduction in grip fatigue, averaging at 56% overall. This is likely because many participants experienced further recovery during their with CASET trial, which when compared to the loss experienced during the empty-handed trial shows significant reduction. The most notable negative during this experiment is the participant which experienced 50% more fatigue when using CASET.

Lastly, participants filled out a standard system usability scale (SUS) on CASET after the experiment [59]. Participant's SUS scores were calculated and are displayed in Fig. 4.19 under the evaluation criteria of [9].

In general, survey responses are in favor of CASET in litter carry operations. The average SUS score of 86.3 displays excellent to best imaginable usability, while also allowing

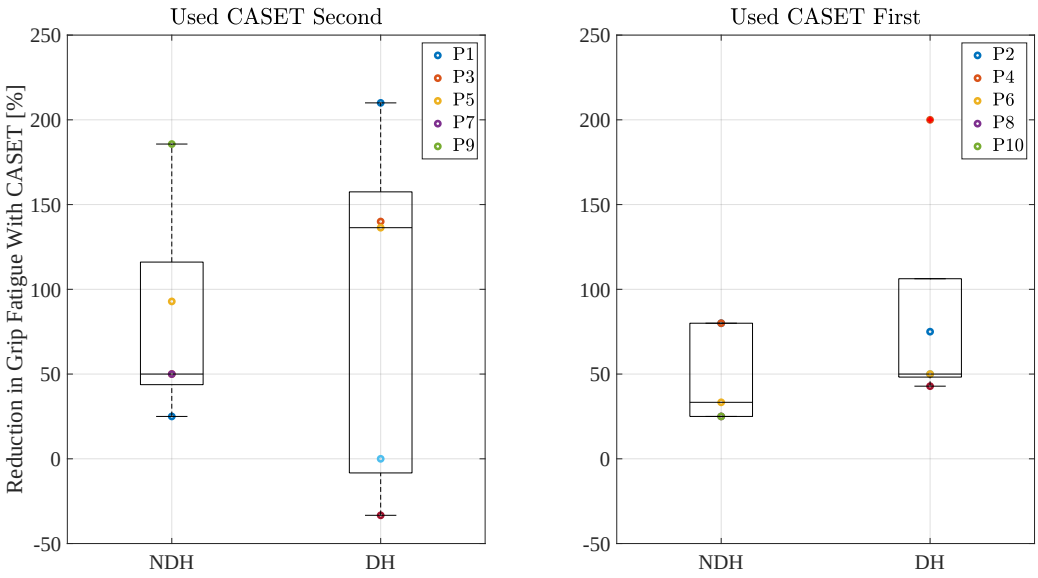

Figure 4.18: Grip fatigue reduction percentage when using CASET to hold the 25lbs weights in the experiment. Dominant hand and non-dominant hand shown respectively as DH and NDH.

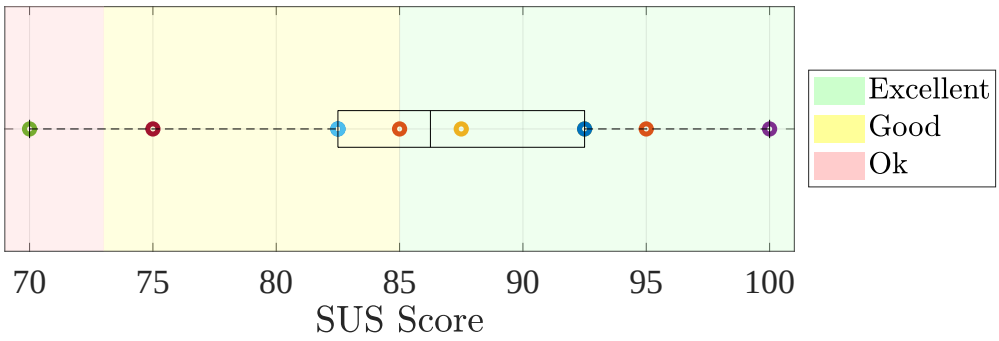

Figure 4.19: System Usability Scale scores per participant. The average score was 86.3±9.3 which falls into the "excellent to best imaginable" category from Bangor et al..

for some improvement to push closer to 100. For comparison, Bangor et al. lists the average SUS from aggregate data at around a 70 with a standard deviation of 21.71. Most participants found the tool easy-to-use and straightforward, but some participants did report that CASET was cumbersome and uncomfortable. It's worth noting that the scale was issued by the researchers responsible for device design, so participants may have been biased in their survey responses. The most common report in the free-response section of the SUS was that

CASET reduced blood flow to the hands and created uncomfortable levels of pressure on the wrists.

While Lewis describes the best metric from the SUS as the final score, individual results of this survey are seen tallied on Table 4.2:

Question	1	2	3	4	5
I think that I would like to use this tool frequently	1		5	2	2
I found the tool unnecessarily complex	10				
I thought the tool was easy to use	1			2	7
I think that I would need the support of a technical person to be able to use this tool	6	4			
I found the various functions in this tool were well integrated			1	3	6
I thought there was too much inconsistency in this tool	7	3			
I would imagine that most people would learn to use this tool very quickly				3	7
I found the tool very cumbersome to use	4	3	2	1	
I felt very confident using the tool				6	4
I needed to learn a lot of things before I could get going with this tool	8	2			

Table 4.2: System Usability Survey (SUS) results for CASET where 1 is "Strongly Disagree" and 5 is "Strongly Agree".

4.3.3 Discussion

With average reduction in grip fatigue for all participants of 56%, the reductions of CASET are in line with the results of the USAARL study in Section 4.1.

The average carry time unassisted was 3:36, and the average carry with CASET was 11:34. This is an improvement average of 320% for all participants, an extraordinary increase which highlights the effectiveness of the device. However, There is a significant deviation from the mean across all participants. P6 and P7, shown as the lowest carry time improvements for each subplot of Fig. 4.17 respectively, both had the lowest increases in carry time.

P6 was an extreme outlier, holding unassisted for 10:11 which is nearly the average time held *with* CASET. P6 still managed to hold with CASET for 17:02, which is 0.75 standard

deviations above the average with CASET, so they still saw significant non-relative increase in carry time. P6 was also the highest weight participant of the group at 99 kg, a sign that outlier heights/weights could experience smaller improvements with CASET.

On the other hand, P7 was the lowest unassisted holder at a time of 1:09. Their with CASET time of 1:41 was the lowest increase (46%) from unassisted to assisted carry. P7 reported on their SUS that they experienced significant loss in blood flow, and stated the gloves used to protect user's hands were potentially too thick and the cause of that feeling. Contrary to P6, P7 was the lightest participant of the study at 50 kg which is yet another sign that physical outliers may experience less improvement when using CASET.

Regarding system usability, all participants noted a significant reduction in stress in the fingertips when using CASET and instead stated how the loads were experienced primarily in the shoulders and trapezius muscles. This is CASET's main objective, and the working principles were mathematically capable of achieving it. Most participants reported the tool as simple and easy-to-use, which are exceptional traits for a device to be used in high-stakes fields where users should not be hindered by their assistive devices. On average, CASET did not perform poorly on any SUS metric, with average scores of strongly agree for traditionally positive metrics (e.g., "I thought the tool was easy to use") and strongly disagree on traditionally negative ones (e.g., "I thought there was too much inconsistency in the tool"). As shown in Fig. 4.19, the participants scored CASET around the "excellent" category the most with an average score of 86.3, meaning while CASET is considered very usable, there is still room for improvement in future versions.

There are a few potential limitations to this study in terms of the environment and measurements. First, the CASET gripper tightness on participants was not directly regulated, instead relying on a 'feels good' remark from the subject. Therefore, some participants reported (on the SUS free-response) a perceived decrease in blood flow to their hands as a result of the pressure felt on their wrists. This blood flow may have limited the fatigue reduction by CASET. The environmental impacts of the study are primarily differences from

it and the study completed by [50]. In this study, it was decided that participants would remain seated and only hold 25lbs dumbbells instead of walking on a treadmill holding 55lbs weights. These decisions were made because, in a pilot test, it was revealed that the participants who were likely not strong enough or as capable as soldiers would barely be able to hold the weights at all. Therefore, to make the study more accessible these constraints were imposed with the understanding that they may impact results. Lastly, it's likely there is a trend between aspects that remained unmeasured, such as hand size, that could impact the improvement one could see from the use of CASET. Future experiments could address these unmeasured aspects.

These results point to the need for an improved CASET version in the future that retains the performance of this version but further emphasizes comfort, specifically in regards to the user's wrists. This could be achieved by widening the contact area around the wrists or adding more padding the the straps that were originally used. Eventually, such a device would need to be compared to other alternatives (like weightlifting hooks) in the same experiment to compare not only improvement over unassisted carry but improvement from one carry method to another.

4.4 The Next Version of CASET

Pilot testing may have reveled CASET was capable of meeting its don/doff requirements and power consumption, but in any case where a service member is carrying extra weight, minimizing said weight is essential. Therefore, a mock up of the actuator for the CASET prototype was generated and can be seen in Fig. 4.20.

This improve actuator is smaller and lighter than the current version whilst retaining all performance.

While this improvement would make CASET significantly better, participants in the experiment still stated they would prefer some more comfort around the wrists. This is achievable through spreading the load on the wrists with extra padding or custom wrist

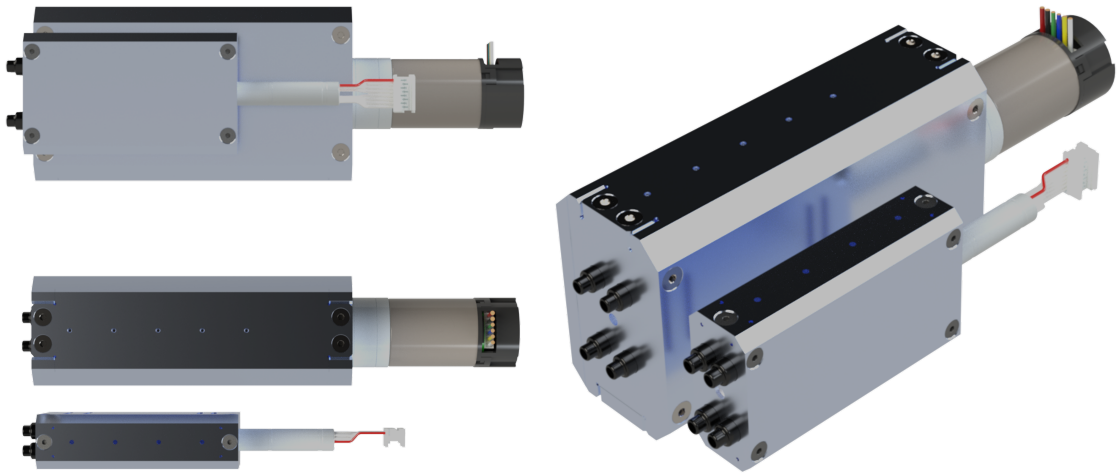

Figure 4.20: Side-by-side comparison of the current CASET actuator and proposed actuator design which uses a brushless DC motor and much smaller overall profile.

straps instead of the off-the-shelf ones used. In the future, working with real litter carry units could unveil more about the design that should be changed to improve performance in the field.

Chapter 5

Human-Interactive Robot Design Discussion

5.1 Robotics Design Guidelines

In robotics design, adhering to general guidelines allows for improved efficiency in the design process and increased fidelity in experimental results. In the cases of both SER and CASET, many design and interfacing techniques were used that should be leveraged in other rehabilitation or assistive devices. Future devices in rehabilitation and assistance should should use a combination of the following design and interfacing principles to generate effective devices.

Prioritizing Safety

For any human-interactive robot, test subjects are going to be cautious and reluctant to freely interact with the device [62]. Therefore, it's important to make the subject as comfortable as possible by properly explaining how safe they device is and providing multiple means of exiting the experiment.

For SER, this was done by providing the user with an easy-to-access E-stop button that would disable the experiment, seen in Fig. 5.1. Subjects were informed they could end the experiment whenever uncomfortable, which helped provide participants with enough comfort to focus their efforts on the experiment itself instead of safety concerns. However, no participant felt the need to activate the E-stop during the experiment.

For CASET, two researchers were actively monitoring the participant as they held weights, and there was significant padding and support provided underneath the participant for when they failed to hold any longer. Participants were informed on how CASET worked, and how it would not move on its own during their experiment. Although the experiment involved holding 'to failure', participants were informed that they may release the

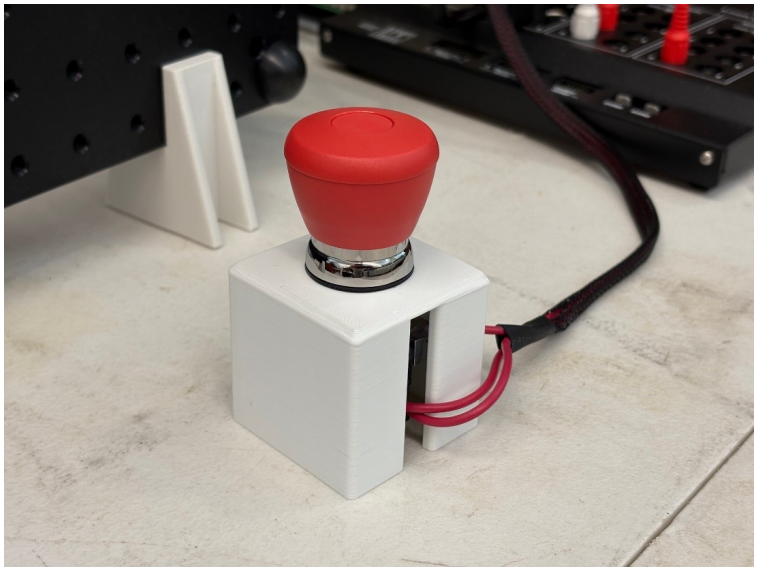

Figure 5.1: The E-stop users were allowed to press during the SER experiment to cut power to the devices in the event of discomfort.

weights whenever they felt uncomfortable. These measures keep the participant in control and allow them to feel more comfortable with the device.

In general, provide participants with ways to exit a device at any time they feel uncomfortable and ensure constant communication with the participant during the experiment to help put them at ease. Naturally, users will feel more comfortable with the system the longer they get to use it for, so extend experiments as needed if comfort is important for data collection.

Work With the Intended Users

To understand the root of a problem and what potential users would like to interface with, it is important to converse with the device's intended user early in the design process. Users may have many reasons to avoid using an assistive device such as: the device being too confusing, too awkward or embarassing to use, or poor environmental fit [63]. Discourse with potential users directs design decisions away from these pitfalls and towards a desirable, usable assistive/rehabilitation device.

Due to a lack of an approachable target audience for either project, SER and CASET did not begin with user-focused design discussions. As a result both designs had issues with

usability that could have been avoided with external feedback. Both designs have since been reviewed by participants, including an open-table discussion with CASET participants and the research team which unveiled bountiful information pertaining to improvements and usability.

For example, RA patients may be asked what how day-to-day is impacted by RA and what elements of a simulation they would find best mimics the feeling. Or, RA patients who experience on one or two fingers but not all may benefit from engaging with a device like SER and comapring that to what the feel on their afflicted fingers.

Ensure the Device is Maintainable and Repairable

To minimize the impact of repeated usage of assistive and rehabilitation focused technologies, it's valuable to build accessible assemblies that may be improved, fixed, or maintained after creation.

For the CASET project, the entire system can be re-cabled by removing only four screws on the linear actuator box. This minimizes the amount of time needed to replace the system which is most likely to need replacement.

On the other hand, SER's capstans can be tensioned up to 5mm per cable end, significantly increasing their lifespan and building in a countermeasure to inevitable cable stretch. The tensioning system for SER can be seen in Fig. 5.2.

Utilize 3D Printing

3D Printing/Additive Manufacturing has allowed for quick turnaround and thorough iteration for both the SER and CASET projects. Seen in subsection 5.1.1, multiple part iterations and 3D prints for SER and CASET were used in both prototyping and final products.

Figure 5.2: A close up of the cable tensioning system for a single SER capstan. tightening the screw increases tension of the cable which allows for adjustability and easy compensation for cable stretch.

5.1.1 3D Printing and the Implications on SER and CASET

The rise of additive manufacturing has allowed for cost and time effective production of complex prototypes in early stages of robot development. These printed parts can be used to validate models or check for errors and allow for more efficient iteration through versions.

While it is still essential to validate the design with models, being able to get hands-on in the earliest stages of device development has been a core part of both SER and CASET. By infusing the rapid prototyping technique of "print early and often", I was able to build and test numerous versions of each device and reached efficient final versions far sooner than I would have through a more traditional "model now, build later" approach.

As discussed in section 2.4, a Prusa Mk4 was used to produce the majority of parts for all versions of CASET and SER. The printer, and an example of how it may slice parts and generate gcode for the printer to read can be seen in Fig. 5.3.

By leveraging available additive manufacturing technologies, costs can be reduced, models can be validated sooner, and a higher number of iterations may be developed on similar timelines. Both SER and CASET were developed with a "print early and often" mindset

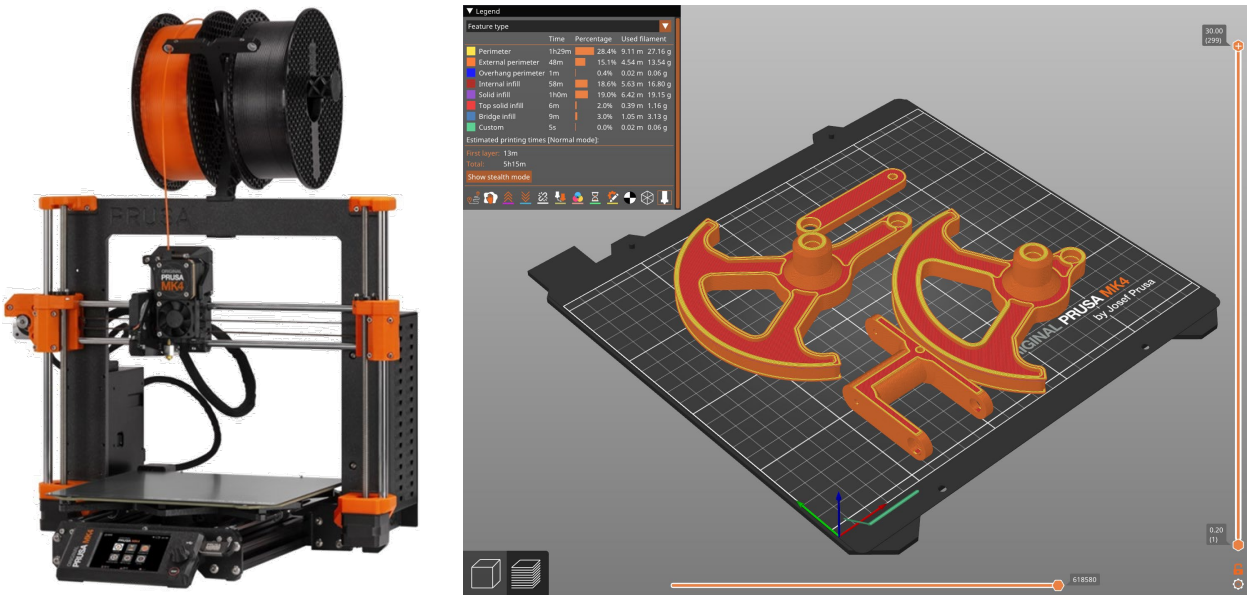

Figure 5.3: (Left) Prusa Mk4, the 3D Printer used for all 3D prints in this manuscript. All prints for SER and CASET are printed with polyactic acid (PLA) at various infill patterns, layer heights, and perimeter numbers. (Right) An example slicing of some SER Version 3.0 prints, layer heights and print estimations shown in-software.

which should be cited as the most crucial part of the protyping process. Human-interactive devices often experience lower loads as well, meaning that final part versions may also be generated from polymer-based materials using AM. Thus, effective use of AM in prototyping and development of human-interactive robots produces improved outcomes with quicker turnaround.

5.2 Robot-to-Human Interfacing Guidelines

Hardware Control and Sampling Rate

Sample time is important when designing robotic systems, and given humans hardly ever move beyond 8.5 Hz [64], many electronic sampling rates are beyond sufficient to capture or control that motion. Understanding both the maximum movement of the region of the user being controlled/observed as well as the frequency detectable by the mechanoreceptors triggered is crucial for selecting appropriate device controllers.

Also, robotic systems often rely on external communication platforms such as user datagram protocol (UDP), transmission control protocol (TCP), or a Robot Operating System (ROS). Attempting to sample/control at a rate too fast for data transmission across these platforms may create delays in those communications and thus the robot control. To minimize or eliminate these issues, understand and select appropriate sampling and control methods.

Similarly, understanding mechanical limitations of the technology is important when multiple devices need to interact with one another. For SER, the HaptX G1 gloves had a mechanical limitation in the highest frequency PWM control being 30Hz. Various modifications to SER's control described in 3.3.3 were done to match the limits of the HaptX, and the absence of these modifications would have significantly impacted the results of the experiment.

Following guidelines set by seminal frequency and sampling papers by those like [65] to mitigate noise and capture all the necessary motion of your subject is key to creating effective robots for human interaction.

Physical Compliance to Users

Humans move organically, and robots do not without intentional modifications to their design. Understanding how to best bridge this gap without completely over-complicating systems through the use of compliant technologies is extremely important when designing human-interactive devices [66].

The best way to do this is provide compliance in the sizing and operation of the device. When able, using soft components like fabric and low durometer polymers allows for seamless integration between human and robot. Both SER and CASET used compliant components to not only improve contact with users but also increase visual comfort by 'softening' external components. SER provided an adjustable hand rest and allowed users to use different sized HaptX gloves to fit various users. CASET complied to a large variety of sized participants

through the inherent flexibility of bowden cables, and could interact with various litter carry handles through the foam padding located on the inside of the grippers.

Transparency and Predictability

Human-interactive Robots should not be unpredictable. Users must be completely confident in what the robot will do in response to their actions to be comfortable in the system. Comfort in a general sense is essential for gathering useful, accurate data points since a user who is comfortable with the devices can focus on the experiment at hand.

For example, in the SER experiment, participants aren't supposed to know exactly which device they are experiencing. However, users were exposed to every possible outcome and encouraged to explore the full ROM of the system before the actual experiment. This allowed participants to be aware of device limitations and thus focus on the binary discretion experiment. In CASET, sufficient explanation of the device and exactly how it worked was done to make sure participants understood what they were doing an how to use the device.

Comfortable patients provide better results and are more willing to participant in unique experiments which must be conducted to understand new technologies [67]. Therefore, ensuring the device is predictable and straightforward is essential for these experiments.

Multimodal Communication

Another way to keep patients comfortable is by communicating all the information they need via different means. Providing audible, haptic, and visual feedback when able may eliminate any worry or doubt the participant might have. Communicating experiment steps through various means also keeps participants on-track and avoids time loss due to miscommunication.

SER utilized a monitor that relayed the current stage of the experiment through a stoplight visual seen in Fig. 5.4 as well as the vibration of SER's endpoint to tactically relay when the data collection was happening. CASET provided visual and auditory feedback to the user with constant updates from the research team as well as a monitor which displayed active data collection and a timer for their carry.

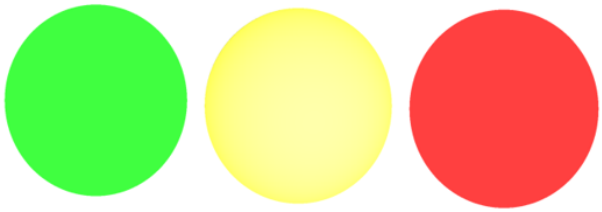

Figure 5.4: The stoplight visual displayed for participants in the SER binary discretion experiment.

Chapter 6

Conclusion and Final Remarks

The future in rehabilitation and assistance lies in human-interactive robotics. To create effective robots capable of meeting design criteria while also being understandable and straightforward for their intended users, exercising smart and collaborative design methodologies is essential. This thesis explored how these design concepts were leveraged in the design of two novel robots: SER and CASET, as well as explored the validation of these robots and how they answer the questions they were intended to.

To create salient virtual simulations of internal effecting diseases like Rheumatoid Arthritis, one must understand if the current state-of-the art (SoTA) haptics technology, which is intended to simulate endpoint object interaction, is capable of generating internal impedance. To test this I developed a novel robotic device (Stiffness Emulation Robot, SER) and compared it to a novel controller on a SoTA haptics glove (HaptX G1). The design and iterations of SER lead to the development of a final version that was used in an experiment where participants differentiated between joint and endpoint experience using touch alone. While the results of this experiment do point towards the need of a novel haptic robot that can generate joint impedance for all five fingers, exploration of pseudo-haptic effects (such as an avatar mismatch to 'show' the impedance) and further testing must be conducted.

On the other hand, the need for assistive robots to improve human capabilities grows stronger as we approach the limits of human ability. Notably, litter carry groups (such as in search-and-rescue operation) experience complex stresses on the musculoskeletal system which cause grip fatigue and leads to eventual failure over extended carry distances. While there are existing means of mitigating these stresses, they lack the ability to retract and remain unobtrusive - a key factor in long term use and adoption. To solve this problem

we developed a novel assistive device: the Curling Artificial Soft ExoskeleTon (CASET), a solution which offloads high loads from the user's fingers to larger muscle groups. Iterations of CASET improved and resulted in a device which was compared to unassisted humans in an experiment where participants held 25lbs weights to failure both with ant without CASET. This experiment, combined system usability reports, revealed that CASET significantly increases carry time and reduces grip fatigue. While it achieves this goal, CASET is not without room for improvement and these results point towards the need to further develop a future version of CASET that emphasizes comfort and usability.

Through pilot experiments to validate the intent and performance of both SER and CASET, working principles such as AM, cables & capstans, PWM, and psychophysics were all shown functioning adequately. However, improvements to both devices and the future in more controlled experiments would also be beneficial in the near future. In both a rehabilitation and assistance space, human-interactive robots like SER and CASET may be utilized in a multitude of future experiments to answer new questions in haptics and assistance.

Bibliography

[1] 3D Systems. Touch haptic device, 2014. URL https://www.3dsystems.com/haptics-devices/touch.

[2] Chad G Rose. *Hybrid Rigid-Soft Exoskeleton Design*. PhD thesis, Rice University, 2018.

[3] Monica Malvezzi, Zubair Iqbal, Maria Cristina Valigi, Maria Pozzi, Domenico Prattichizzo, and Gionata Salvietti. Design of multiple wearable robotic extra fingers for human hand augmentation. *Robotics*, 8(4):102, 2019.

[4] Chang Liu, Dahai Wang, Puning Chen, Yangming Xie, and Janet Dong. Design a wearable exoskeleton to free litter bearers' hands and achieve multi-task capabilities for casualty evacuation. In *ASME International Mechanical Engineering Congress and Exposition*, volume 88636, page V005T07A026. American Society of Mechanical Engineers, 2024.

[5] Maxon. Dc motor (339152), 2023. URL https://www.maxongroup.com/maxon/view/product/motor/dcmotor/re/re25/339152.

[6] Pololu. Dc motor (4846), 2024. URL https://www.pololu.com/product/4846.

[7] AMC. Cb12a1c motor driver (discontinued), 2023. URL https://www.a-m-c.com/.

[8] Pololu. Drv8874 motor driver (4035), 2024. URL https://www.pololu.com/product/4035.

[9] Aaron Bangor, Philip T Kortum, and James T Miller. An empirical evaluation of the system usability scale. *Intl. Journal of Human–Computer Interaction*, 24(6):574–594, 2008.

[10] Gowri Shankar Giri, Yaser Maddahi, and Kourosh Zareinia. An application-based review of haptics technology. *Robotics*, 10(1):29, 2021.

[11] Lucian Panait, Ehab Akkary, Robert L Bell, Kurt E Roberts, Stanley J Dudrick, and Andrew J Duffy. The role of haptic feedback in laparoscopic simulation training. *Journal of Surgical Research*, 156(2):312–316, 2009.

[12] Kenneth O Johnson. The roles and functions of cutaneous mechanoreceptors. *Current opinion in neurobiology*, 11(4):455–461, 2001.

[13] Robert J Stone. Haptic feedback: A brief history from telepresence to virtual reality. In *International Workshop on Haptic Human-Computer Interaction*, pages 1–16. Springer, 2000.

[14] Tyler Rose, Chang S Nam, and Karen B Chen. Immersion of virtual reality for rehabilitation-review. *Applied ergonomics*, 69:153–161, 2018.

[15] Anatole Lécuyer, Sabine Coquillart, Abderrahmane Kheddar, Paul Richard, and Philippe Coiffet. Pseudo-haptic feedback: Can isometric input devices simulate force feedback? In *Proceedings IEEE Virtual Reality 2000 (Cat. No. 00CB37048)*, pages 83–90. IEEE, 2000.

[16] Mingyu Kim, Changyu Jeon, and Jinmo Kim. A study on immersion and presence of a portable hand haptic system for immersive virtual reality. *Sensors*, 17(5):1141, 2017.

[17] Samuel T McJunkin, Marcia K O'Malley, and John E Speich. Transparency of a phantom premium haptic interface for active and passive human interaction. In *American Control Conference, 2005*, pages 3060–3065. IEEE, 2005.

[18] HaptX Inc. HaptX Gloves G1, 2024. URL `https://haptx.com/gloves-g1/`.

[19] Domenico Prattichizzo, Maria Pozzi, Tommaso Lisini Baldi, Monica Malvezzi, Irfan Hussain, Simone Rossi, and Gionata Salvietti. Human augmentation by wearable supernumerary robotic limbs: review and perspectives. *Progress in Biomedical Engineering*, 3(4):042005, 2021.

[20] Federico Parietti and Harry Asada. Supernumerary robotic limbs for human body support. *IEEE Transactions on Robotics*, 32(2):301–311, 2016.

[21] Irfan Hussain, Gionata Salvietti, Giovanni Spagnoletti, and Domenico Prattichizzo. The soft-sixthfinger: a wearable EMG controlled robotic extra-finger for grasp compensation in chronic stroke patients. *IEEE Robotics and Automation Letters*, 1(2):1000–1006, 2016.

[22] Ragita C Pramudya and Han-Seok Seo. Hand-feel touch cues and their influences on consumer perception and behavior with respect to food products: A review. *Foods*, 8 (7):259, 2019.

[23] Uwe Proske. Kinesthesia: the role of muscle receptors. *Muscle & Nerve: Official Journal of the American Association of Electrodiagnostic Medicine*, 34(5):545–558, 2006.

[24] Melissa K Stern and James H Johnson. Just noticeable difference. *The corsini encyclopedia of psychology*, pages 1–2, 2010.

[25] Gustav Theodor Fechner. Elements of psychophysics, 1860. 1948.

[26] Tom N Cornsweet. The staircase-method in psychophysics. *The American journal of psychology*, 75(3):485–491, 1962.

[27] Zefeng Yan, Haoyuan Yi, Zihao Du, Tiantian Huang, Bin Han, Lufeng Zhang, Ansi Peng, and Xinyu Wu. Development of an assist upper limb exoskeleton for manual handling task. In *2019 IEEE International Conference on Robotics and Biomimetics (ROBIO)*, pages 1815–1820. IEEE, 2019.

[28] Michael M Starkey and Robert L Williams. Capstan as a mechanical amplifier. In *International Design Engineering Technical Conferences and Computers and Information in Engineering Conference*, volume 54839, pages 1309–1316, 2011.

[29] Andre Schiele, Pierre Letier, Richard Van Der Linde, and Frans Van Der Helm. Bowden cable actuator for force-feedback exoskeletons. In *2006 IEEE/RSJ International Conference on Intelligent Robots and Systems*, pages 3599–3604. IEEE, 2006.

[30] Amanpreet Singh and Jitendra P Khatait. Mechanism for tension adjustment in tendon driven remote center-of-motion mechanism for minimally invasive surgery. *Proceedings of the Institution of Mechanical Engineers, Part C: Journal of Mechanical Engineering Science*, 236(16):9293–9305, 2022.

[31] Jagwire. DIY Brake Kit, 2017. URL `https://jagwire.com/products/diy-cable-kits/2017road-elite-link-brake-kit/`.

[32] Syed AM Tofail, Elias P Koumoulos, Amit Bandyopadhyay, Susmita Bose, Lisa O'Donoghue, and Costas Charitidis. Additive manufacturing: scientific and technological challenges, market uptake and opportunities. *Materials today*, 21(1):22–37, 2018.

[33] Ramu Krishnan. Electric motor drives—modeling, analysis, and control. *IEEE Press*, 2001.

[34] Alex Ellin and Gregor Dolsak. The design and application of rotary encoders. *Sensor Review*, 28(2):150–158, 2008.

[35] Brad Paden and Ravi Panja. Globally asymptotically stable 'pd+'controller for robot manipulators. *International Journal of control*, 47(6):1697–1712, 1988.

[36] Neville Hogan. Impedance control: An approach to manipulation: Part ii—implementation. *JDSMC*, pages 8–16, 1985.

[37] Bruno Siciliano. Kinematic control of redundant robot manipulators: A tutorial. *Journal of intelligent and robotic systems*, 3:201–212, 1990.

[38] Kimberly B Garza et al. Assessing the effectiveness of virtual reality to promote empathy for patients through a mixed-methods study. *American Journal of Pharmaceutical Education*, 88(6):100702, 2024.

[39] Maria Moudatsou, Areti Stavropoulou, Anastas Philalithis, and Sofia Koukouli. The role of empathy in health and social care professionals. *Healthcare*, 8(1), 2020.

[40] Uli Bromberg, Maria Lobatcheva, and Jan Peters. Episodic future thinking reduces temporal discounting in healthy adolescents. *PLoS One*, 12(11):e0188079, 2017.

[41] Heather Culbertson, Samuel B Schorr, and Allison M Okamura. Haptics: The present and future of artificial touch sensation. *Annual review of control, robotics, and autonomous systems*, 1(1):385–409, 2018.

[42] Prusa. Mk4s 3d printer, 2023. URL `https://www.prusa3d.com/category/original-prusa-mk4s/`.

[43] Jorge Angeles. *Fundamentals of robotic mechanical systems: theory, methods, and algorithms*. Springer, 2003.

[44] Jean-Pierre Merlet. Jacobian, manipulability, condition number, and accuracy of parallel robots. *Journal of Mechanical Design*, 2006.

[45] Pietro Morasso. Spatial control of arm movements. *Experimental brain research*, 42(2): 223–227, 1981.

[46] Susan J Lederman and Roberta L Klatzky. Extracting object properties through haptic exploration. *Acta psychologica*, 84(1):29–40, 1993.

[47] Hubert R Dinse, Tobias Kalisch, Patrick Ragert, Burkhard Pleger, Peter Schwenkreis, and Martin Tegenthoff. Improving human haptic performance in normal and impaired

human populations through unattended activation-based learning. *ACM Transactions on Applied Perception (TAP)*, 2(2):71–88, 2005.

[48] Youngmok Yun, Sarah Dancausse, Paria Esmatloo, Alfredo Serrato, Curtis A Merring, Priyanshu Agarwal, and Ashish D Deshpande. Maestro: An emg-driven assistive hand exoskeleton for spinal cord injury patients. In *2017 IEEE international conference on robotics and automation (ICRA)*, pages 2904–2910. IEEE, 2017.

[49] Priyanshu Agarwal and Ashish D Deshpande. Subject-specific assist-as-needed controllers for a hand exoskeleton for rehabilitation. *IEEE Robotics and Automation Letters*, 3(1):508–515, 2017.

[50] Adrienne M Madison, Tamara T Chambers, Alexis S Stewart, and V. C. Chancey. Evaluation of litter carriage performance and post-carry fatigue effects in prolonged combat field care environments (part 1): Preliminary design considerations, specifications, and recommendations for exoskeleton feasibility, suitability, and efficacy in dismounted military casualty transport scenarios. Technical Report, Final Report AD1182730, Army Aeromedical Research Laboratory; Oak Ridge Institute for Science and Education, 2024. URL `https://apps.dtic.mil/sti/citations/AD1182730`. Accession Number: AD1182730.

[51] Valerie JB Rice, Marilyn A Sharp, William J Tharion, and Tania L Williamson. The effects of gender, team size, and a shoulder harness on a stretcher-carry task and post-carry performance. part i. a simulated carry from a remote site. *International Journal of Industrial Ergonomics*, 18(1):27–40, 1996.

[52] Wayne WILLIAMS. Carbonhand from bioservo, 2022.

[53] Johan Ingvast, Hans Von Holst, and Jan Wikander. Strengthening glove, October 4 2011. US Patent 8,029,414.

[54] Harbinger. Lifting hooks, 2024. URL https://www.roguefitness.com/harbinger-lifting-hooks.

[55] Aoife Finneran and Leonard O'Sullivan. Effects of grip type and wrist posture on forearm emg activity, endurance time and movement accuracy. *International Journal of Industrial Ergonomics*, 43(1):91–99, 2013.

[56] Sen Qian, Bin Zi, Wei-Wei Shang, and Qing-Song Xu. A review on cable-driven parallel robots. *Chinese Journal of Mechanical Engineering*, 31(1):1–11, 2018.

[57] Edoardo Idà and Valentina Mattioni. Cable-driven parallel robot actuators: state of the art and novel servo-winch concept. In *Actuators*, volume 11, page 290. MDPI, 2022.

[58] Raspberry. Pi pico, 2021. URL https://www.raspberrypi.com/products/raspberry-pi-pico/.

[59] James R Lewis. The system usability scale: past, present, and future. *International Journal of Human–Computer Interaction*, 34(7):577–590, 2018.

[60] Gianluca De Luca. Fundamental concepts in EMG signal acquisition. *Copyright Delsys Inc*, 2003.

[61] George F Hamilton, Carolyn McDonald, and Thomas C Chenier. Measurement of grip strength: validity and reliability of the sphygmomanometer and jamar grip dynamometer. *Journal of Orthopaedic & Sports Physical Therapy*, 16(5):215–219, 1992.

[62] Alessandra Sciutti, Martina Mara, Vincenzo Tagliasco, and Giulio Sandini. Humanizing human-robot interaction: On the importance of mutual understanding. *IEEE Technology and Society Magazine*, 37(1):22–29, 2018.

[63] Laura N Gitlin. Why older people accept or reject assistive technology. *Generations: Journal of the American Society on Aging*, 19(1):41–46, 1995.

[64] R. McNeill Alexander. Simple models of human movement. *Applied Mechanics Reviews*, 48(8):461–470, 1995.

[65] Claude E Shannon. Communication in the presence of noise. *Proceedings of the IRE*, 37(1):10–21, 1949.

[66] Diego Torricelli, Jose Gonzalez, Maarten Weckx, René Jiménez-Fabián, Bram Vanderborght, Massimo Sartori, Strahinja Dosen, Dario Farina, Dirk Lefeber, and Jose L Pons. Human-like compliant locomotion: state of the art of robotic implementations. *Bioinspiration & biomimetics*, 11(5):051002, 2016.

[67] Yuchen Yan and Yunyi Jia. A review on human comfort factors, measurements, and improvements in human–robot collaboration. *Sensors*, 22(19):7431, 2022.

Appendix

A repository of all CAD and code files as well as individual participant SUS surveys for each experiment can be found in the following Auburn University Box folder:

`https://auburn.box.com/s/30pb03xrwuunwzi81byedczck0lsfw75`

Figure 1: QR Code for access to the SER and CASET repository.